The Doubled CO_2 Climate: Impact of the Sea Surface Temperature Gradient

DAVID RIND

Goddard Space Flight Center, Institute for Space Studies, New York, NY 10025

(Manuscript received 17 December 1986, in final form 21 May 1987)

ABSTRACT

Even though five different general circulation models are all currently producing about a 4° ± 1°C warming for doubled CO_2, there is still substantial model disagreement about the degree of high latitude amplification of the surface temperature change. The consequences of this disagreement are investigated by comparing doubled CO_2 climates with different latitudinal gradients of sea surface temperature. The GISS 4° × 5° general circulation model (GCM) was run with doubled CO_2 and two sets of sea surface temperatures: one set derived from the equilibrium doubled CO_2 run of the 8° × 10° GISS GCM, with minimal high latitude amplification, and the other set more closely resembling the GFDL results, with greater amplification. While the experiments differ in their latitudinal distribution of warming, they have the same global mean surface air temperature change. The differences in energy balance, atmospheric dynamics and regional climate simulations are discussed.

The results show that the two experiments often produce substantially different climate characteristics. With reduced high latitude amplification, and thus more equatorial warming, there is a greater increase in specific humidity and the greenhouse capacity (the concentration of infrared-absorbing gases) of the atmosphere, resulting in a warmer atmosphere in general. Features such as the low latitude precipitation, Hadley cell intensity, jet stream magnitude and atmospheric energy transports all increase compared to the control run. In contrast, these features all decrease in the experiment with greater high latitude amplification. There are also significant differences in the cloud cover and stationary eddy energy responses between the two experiments, as well as most regional climate changes; for example, there is greater drying of the midlatitude summer continents and greater polar ice melting when the high latitude amplification is greater. Predictions of the coming doubled CO_2 climate and its societal consequences must be tempered by the current uncertainty in the degree of high latitude amplification.

1. Introduction

A major uncertainty associated with our attempts to predict the doubled CO_2 climate concerns the extent to which low latitudes will warm. Different climate models produce different degrees of low latitude warming, or different magnitudes of high latitude amplification. For example, the Goddard Institute for Space Studies (GISS) model (Hansen et al., 1984) produces a surface air temperature warming of 9.4°C at high northern latitudes during winter, with equatorial warming of about 3.9°C, an amplification of 2.4. The latest Geophysical Fluid Dynamics Laboratory (GFDL) model result (Manabe and Wetherald, 1986; Schlesinger and Mitchell, 1985, 1987) obtains high latitude/low latitude warming of 14°C/2.5°C, an amplification of 5.6. The doubled CO_2 experiment with the NCAR CCM (Washington and Meehl, 1984) found warming of 7°C/3°C, an amplification of 2.33. The differences among the models can perhaps be traced to particular parameterizations, such as the penetrative convection process and the specified ocean transports in the GISS model, or vertical diffusion in the NCAR model. It is important to determine which high latitude amplification is more likely and to understand the consequences of the different latitudinal temperature gradients.

To address the first question, one may look at the paleoclimate record, in particular, at the climate of the last ice age (circa 18 000 years before the present). The CLIMAP (Climate: Long-Range Investigation, Mapping and Prediction Project, 1981) reconstruction indicated that equatorial ocean temperatures cooled by only 1°–2°C, while the existence of glaciers at upper midlatitudes is sufficient proof of intense cooling in the extratropics. This would seem to support the view that significant high latitude amplification is a characteristic feature of the climate system, at least for cooler climates. However, as noted by Rind and Peteet (1985), terrestrial evidence at low latitudes seems to imply that low latitude cooling was much larger than indicated by the CLIMAP reconstruction (for example, glaciers appeared to descend by about 1 km at all latitudes). This uncertainty in the climate record precludes firmly establishing the proper magnitude of high latitude amplification. In addition, differences in cryospheric feedback processes between warm and cold climates make it unlikely that the amplification would be similar in different climate regimes, so the ice age result may be a poor analogy for conditions in a future warming. There is insufficient quantitative paleoclimate evidence regarding past warm epochs (e.g., Mesozoic) to determine the amplification at those times, although high

latitudes appear to have been very warm (e.g., Frakes, 1979).

Alternatively, calculations could be made with coupled dynamical atmosphere–ocean models, which allow the ocean circulation to vary in their determination of the latitudinal sea surface temperature change. Recent simulations of the doubled CO_2 climate with such models have been reported by Manabe and Bryan (1985) for the GFDL model (using prescribed cloud cover, thus different from the GFDL model referred to above) and by Schlesinger et al. (1985) with the Oregon State University (OSU) model. The GFDL result produced a high latitude amplification of about 4.5, while the OSU result, although not fully run to equilibrium, showed an amplification of about 2.5, so the difference remains. The joint models are likely driven in this regard by the characteristics of the atmospheric models, and, combined with uncertainties in ocean models themselves, such models are not yet capable of providing definitive indications of ocean surface temperature changes.

Given this state of affairs, it is not possible at this time to decide the likely magnitude of high latitude amplification of future climate changes. Of primary importance for regional climate forecasts are the consequences of different high latitude amplification. The low latitude hydrologic cycle and Hadley Cell are sensitive to the tropical sea surface temperature distribution (e.g., Rind and Rossow, 1984), so they will vary with the degree of low latitude warming. Baroclinic instability depends on the magnitude of available potential energy, a direct reflection of the latitudinal temperature gradient, and quasi-geostrophic linear theory relates this gradient to instability scales (e.g., Green, 1960). Thus, dynamical quantities at all latitudes will likely be affected by the relative warming of high and low latitudes and, as a result, produce differences in regional climate characteristics and climate change impacts. It is this topic which is explicitly addressed in the present study.

Several previous papers have addressed this issue indirectly. Using the United Kingdom Meteorological Office (UKMO) model, Mitchell (1983) and Mitchell and Lupton (1984) simulated a $2 \times CO_2$ experiment with uniform sea surface temperatures, and a $4 \times CO_2$ experiment with the GFDL sea surface temperatures determined from a $4 \times CO_2$ run. Changes in precipitation between the two experiments were noted, but the major differences were likely due to the greater warming, by a factor of two, in the second experiment. A comparison between simulations of the doubled CO_2 climate and the climate of the Mesozoic (Rind, 1986) depicted how warm climates with different gradients had certain atmospheric dynamical differences, but the comparison was complicated by the different topography that also existed.

In this study we avoid such additional factors by comparing doubled CO_2 climates as simulated in the GISS model using two different sea surface temperature change distributions. The ocean temperature changes chosen produce differences in high latitude amplification similar to the differences between the GISS and GFDL models. As such, they represent the range in current doubled CO_2 model results. The energy balance in the two runs is examined, in an attempt to gain some insight into processes or parameterizations that might be producing the different degrees of high latitude amplification. We explore how atmospheric dynamical quantities change from the control run in each simulation, and how these changes relate to those produced in other climate simulations. Finally, we examine how regional climate patterns, such as the possible summer drying of midlatitude continents, depend on the different latitudinal temperature gradients.

2. Experiments

The model used for these experiments is the GISS GCM (Hansen et al., 1983) run with $4° \times 5°$ resolution and nine vertical levels. This is finer resolution than that used in the doubled CO_2 experiment ($8° \times 10°$) reported by Hansen et al. (1984) and is more appropriate for investigating regional changes. Selected output from this model was shown by Hansen et al. (1983). Its primary deficiencies are excessive rainfall at 12°N in January, a weaker than observed Walker circulation, and somewhat excessive rainfall over the polar ice sheets. The sea level pressure pattern, Ferrel cell, kinetic energy spectrum, eddy momentum transport and movement of synoptic-scale systems are all better than that produced by the coarser resolution model (Hansen et al., 1983).

The control run incorporated the sea surface temperatures averaged over years 26–35 from the coarse grid control run, with CO_2 at 315 ppm, interpolated to the finer resolution. The ocean temperatures are the equilibrium values of the coarse grid model for the current climate and are quite comparable to the observed sea surface temperatures. This is due to the inclusion of specified ocean heat transports that allow the standard simulation to reproduce the current ocean temperatures (Hansen et al., 1984). The "2CO2" experiment used the interpolated sea surface temperatures from years 26–35 of the doubled CO_2 experiment with the coarse grid, at which point the coarse grid model was in energy balance equilibrium, and a CO_2 level of 630 ppm. An alternate doubled CO_2 experiment (ALT) used a sea surface temperature change from the control run chosen to be more in accord with the GFDL doubled CO_2 result (Manabe and Wetherald, 1986), and 630 ppm CO_2. There was no attempt to make the sea surface temperature change correspond precisely to the GFDL result; the alteration of the sea surface temperatures simply changed the latitudinal average warming and the high latitude amplification and so maintained the longitudinal gradients generated by the standard

doubled CO_2 run. When the alterations increased the ocean temperature above the freezing point of −1.6°C, sea ice was decreased; at upper midlatitudes, ALT had about 5% less sea ice than 2CO2. Note that neither of the experiments is in energy balance, since the sea surface temperatures were not generated self-consistently.

The control run and each experiment were run for three and one-half years with an annual cycle, from initial conditions generated by a several year run. Results will be presented for the last three years. While most of the changes described below are large enough to preclude any question of their significance, some of the regional differences are more uncertain statistically, given the possibility of seasonal persistence. In all cases an attempt will be made to understand the changes in terms of the physics of the system, which should minimize this difficulty.

The change in the sea surface temperatures from the control run for the two experiments is presented in Fig. 1 as a function of latitude for the winter and summer seasons. The high latitude amplification (60°/0° latitude) in sea surface temperature change in ALT is more than twice as large as in 2CO2; however, the values were chosen so as to produce a global mean temperature change of 4.2°C in both runs (as produced in the coarse grid runs). The consequences of the difference in the resulting latitudinal gradients to the doubled CO_2 climate are explored in the next section.

3. Results

a. Energy balance

The corresponding surface air temperature changes for the two seasons are shown in Fig. 2. The increased high latitude amplification in ALT is apparent, and the results resemble those of the GFDL experiment, at least for winter (defined here in terms of the Northern Hemisphere season, December–February). The change in the zonally averaged temperature as a function of altitude is given in Fig. 3. The upper panel shows the 2CO2 tropical upper troposphere peak, characteristic of the GISS model doubled CO_2 model result. The middle panel shows the reduced tropical upper troposphere warming in ALT, qualitatively similar to the GFDL result. Schlesinger and Mitchell (1985) speculated that the difference in upper troposphere temperature change between the two models might be due to the more penetrative convection in the GISS model. This may be true in models run to equilibrium, i.e., those that develop their own sea surface temperatures; the results from this study show that it is directly related to the sea surface temperature changes in the model, since both runs use the same convective scheme. The change in the vertical redistribution of heat due to moist convection (Fig. 4) indicates that the warmer sea surface temperatures in 2CO2 lead to substantial increases in high altitude heating. Accompanying the increased moist convective heating is an increase in moisture (shown below), which will also amplify tropical temperature changes.

Annual averages for the relevant quantities are given in Table 1. Included are both surface quantities (when specifically stated) and vertically integrated atmospheric values. Note that although the annual average surface air temperature changes were the same in the two runs, 2CO2 was almost 1°C warmer for the atmosphere as a whole.

How do the sea surface temperature differences affect the radiative properties of the atmosphere? The annual average changes in specific humidity (Fig. 5, left) are positive in both doubled CO_2 experiments, but much greater in 2CO2 at low latitudes due to the warmer temperatures and greater convective activity (which transports more moisture vertically). At higher latitudes the values in ALT are larger, for the same reasons. The global average specific humidity is somewhat greater in 2CO2, which is consistent with its warmer atmospheric temperature. The relative humidity changes (Fig. 5, right) show a more complicated pattern, with generally small increases in both experiments. There is some tendency for 2CO2 to have larger relative humidity values near the equator, especially at high altitudes.

The annual average change in cloud cover is shown in Fig. 6. Comparison with the relative humidity change reveals an odd effect. The 2CO2 run with its increase in upper troposphere relative humidity experiences a large decrease in cloud cover in the same region, affecting primarily large-scale supersaturation clouds. This is an apparent contradiction, since this cloud cover is dependent upon relative humidity, with a sub–grid scale temperature variance extrapolated from the resolvable scale applied to determine what fraction of the grid box would be supersaturated. As noted by Mitchell et al. (1987), the relative humidity and cloud cover changes in the UKMO model are also somewhat poorly correlated; they suggest that this arises because the relative humidity is well below the saturation value, so that small increases in relative humidity may have little effect on supersaturation clouds. The cloud cover reduction may arise as increased convection results in increased subsidence drying in regions with previous cloudiness, with convective moistening occurring in regions where cloud cover was already complete (as suggested by Wetherald and Manabe, 1980, to explain relative humidity decreases in regions of increased vertical velocity variance).

Consistent with its similarity in high latitude amplification to the GFDL simulation, ALT has cloud cover changes that are in qualitative agreement with the latest GFDL result (Schlesinger and Mitchell, 1985). Both experiments show a general reduction in clouds in the tropics and a reduction in middle and low level cloud in midlatitudes. Both show increases in upper level clouds in the extratropics and in low level clouds at the highest latitudes. One difference which does occur

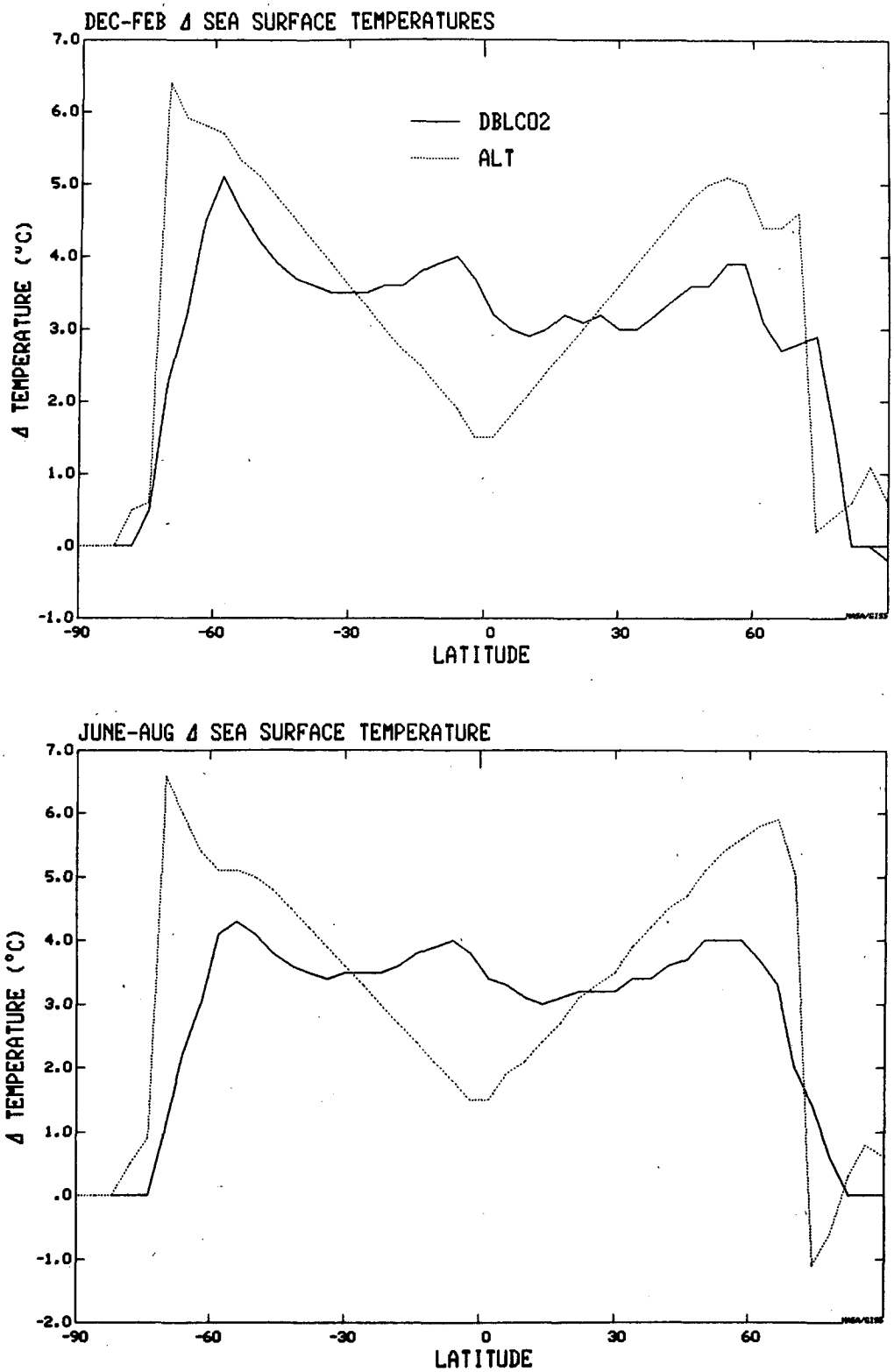

FIG. 1. Difference in specified sea surface temperatures, 2CO2 minus control (solid line), and ALT minus control (dotted line) for the three-year averages of December–February and June–August.

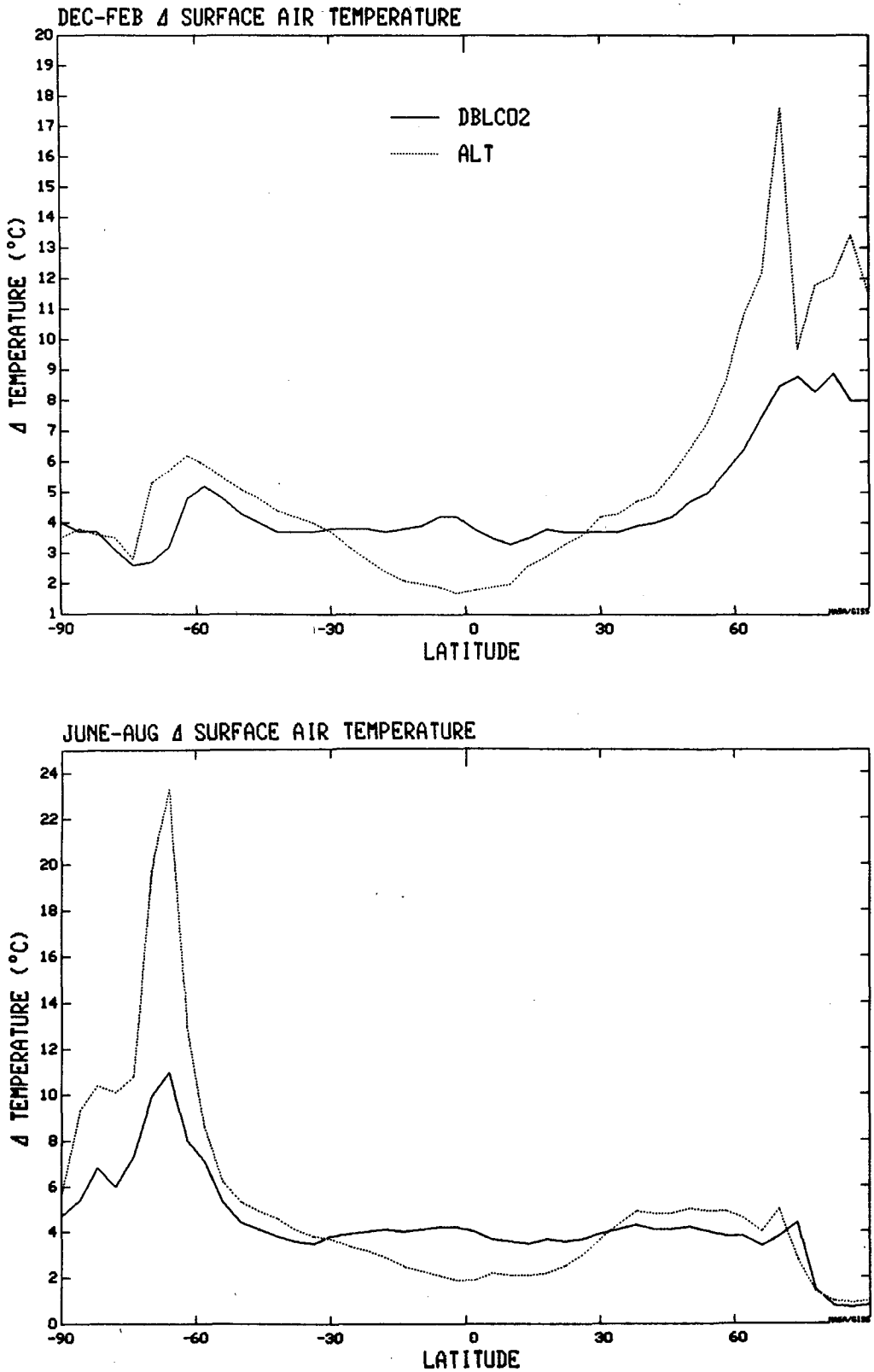

FIG. 2. As in Fig. 1, except for surface air temperature.

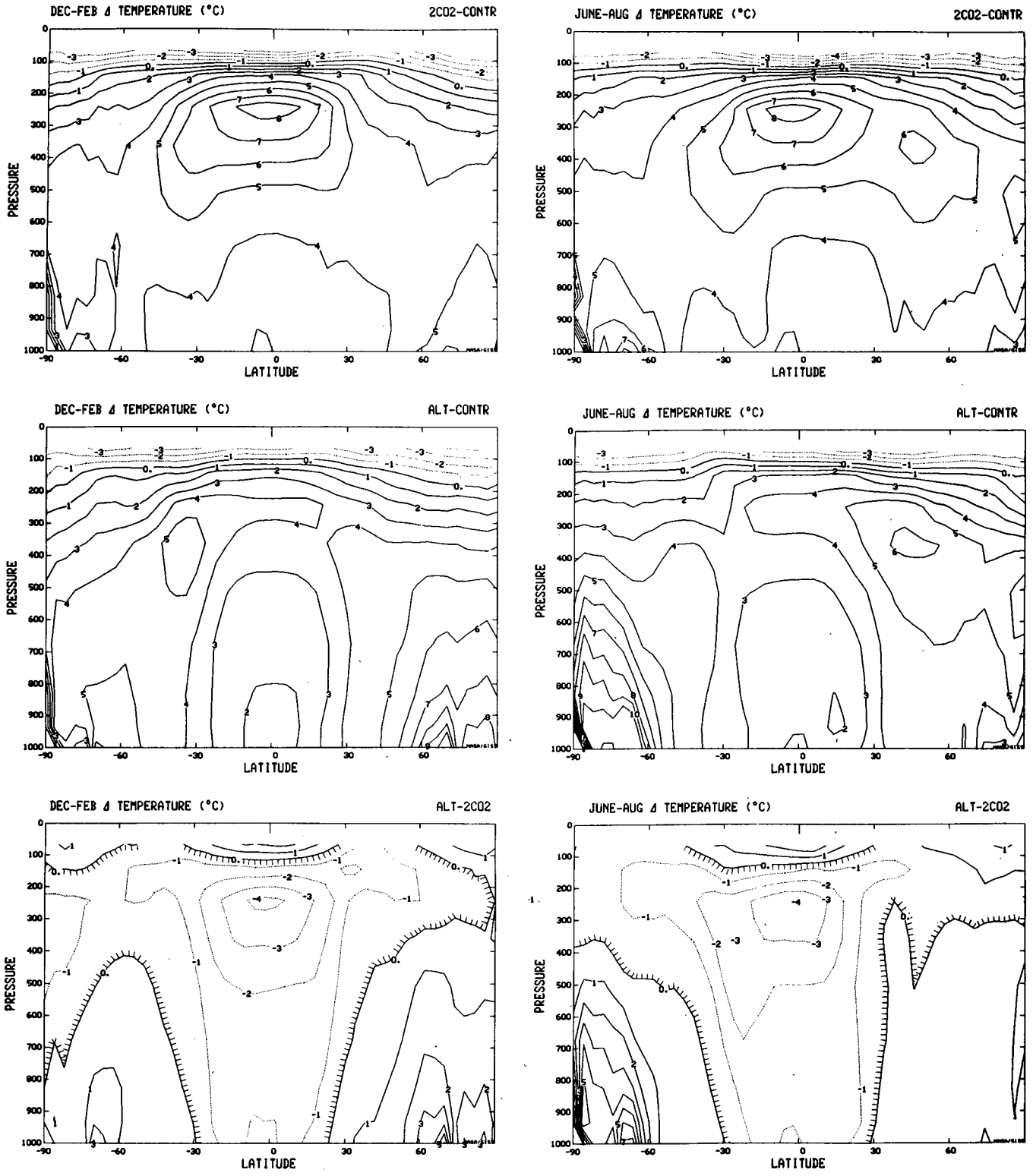

FIG. 3. Change of temperature, latitude versus pressure, for 2CO2 minus control, ALT minus control, and ALT minus 2CO2 from the three-year averages of December–February and June–August.

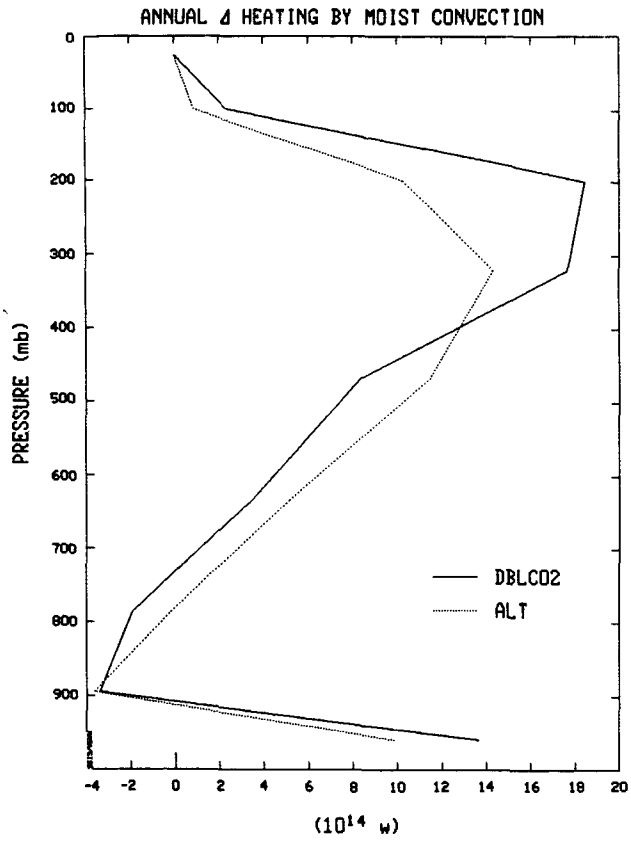

FIG. 4. Global, annual average change in heating by moist convection as a function of pressure, for 2CO2 minus control (solid line) and ALT minus control (dotted line).

is that the GFDL model gets increased cloud cover in the tropics above 100 mb; in the GISS model clouds are not permitted to form in the two highest levels, a deficiency that also is present in the NCAR and UKMO models (Mitchell et al., 1987).

The annual average ground albedo (Fig. 7) decreases more in ALT at higher latitudes, as the warmer high latitude temperatures result in less snow and sea ice. Planetary albedo changes also occur (Fig. 7), but are muted due to the relatively small cloud cover differences. The cloud cover and albedo changes result in differences in shortwave energy absorbed at the surface (Fig. 8), with a greater increase in absorption at mid- and high latitudes in ALT (albedo effect), and a greater low latitude increase in 2CO2 (due to cloud cover decrease). The net longwave radiation received at the surface (Fig. 8) is greater in 2CO2 everywhere due to the increase in specific humidity and CO_2; at higher latitudes in ALT the strong surface warming overcomes this effect and the net longwave energy decreases. The net radiation change at the surface (Fig. 8) thus shows similar increases in the extratropics in both experiments (as the shortwave and longwave changes compensate), but much greater increase in the tropics in 2CO2.

The net heating at the surface is the sum of the net radiation and the net surface fluxes. ALT had warmer sea surface temperatures in the tropics than did the control run, but the tropical change represented the minimum increase when compared with other latitudes (Fig. 1). As shown in previous climate model simulations (Rind 1986, 1987), regions of minimum sea surface temperature increase are regions of decreased evaporation, regardless of the absolute magnitude of warming, due to changes in circulation induced by the new sea surface temperature pattern. ALT therefore has less energy loss due to surface fluxes (Fig. 9), while the maximum sea surface temperature change near the equator in 2CO2 produced a large increase in surface energy loss. This difference more than offsets the difference in net radiative heating of the surface and provides ALT with surplus heat in the equatorial region (Fig. 9). The result is simply a demonstration of the fact that the model in equilibrium for doubled CO_2 does not produce such cool sea surface temperatures in the tropics and would warm if allowed. As shown below, it also indicates that an implicit ocean heat transport divergence in the tropics is occurring in ALT to generate the specified sea surface temperatures. Some high latitudes in ALT experience a net loss of energy from the surface, due to the intense surface fluxes associated with decreased sea ice. This, again, would be expected, as the standard model does not produce such high latitude amplification. The net cooling in the tropics for 2CO2 implies that the finer grid model used in these experiments might have produced somewhat cooler tropical sea surface temperatures if it were allowed to run to equilibrium. The control run evaporation, and the change in evaporation due to doubled CO_2, are somewhat greater in the fine grid runs, at least partially a result of greater surface winds in the fine grid control.

b. Atmospheric dynamics

Results shown here are for the Northern Hemisphere winter season, with its vigorous circulation. Northern

TABLE 1. Annual average global results.

Climate variable	Control	2CO2	ALT
Sea surf temp (°C)	20.1	23.1	22.7
Surf air temp (°C)	14.3	18.6	18.6
Vert-int air temp (°C)	−20.3	−16.3	−17.1
Moist conv heating (10^{14} W)	456.5	511.6	502.1
Specific humidity (10^{-5})	265.3	352.3	331.8
Relative humidity (%)	44.4	46.2	45.7
Cloud cover (%)	49.9	44.6	46.7
Ground albedo (%)	11.3	10.4	10.1
Planetary albedo (%)	28.2	26.5	26.1
Shortwave abs at surf (W m^{-2})	178.3	182.2	183.7
Net longwave at surf (W m^{-2})	−49.7	−45.4	−47.9
Net radiation at surf (W m^{-2})	128.6	136.9	135.8
Net surf fluxes (W m^{-2})	−124.3	−132.5	−128.6
Net heating at surf (W m^{-2})	3.2	3.5	6.4

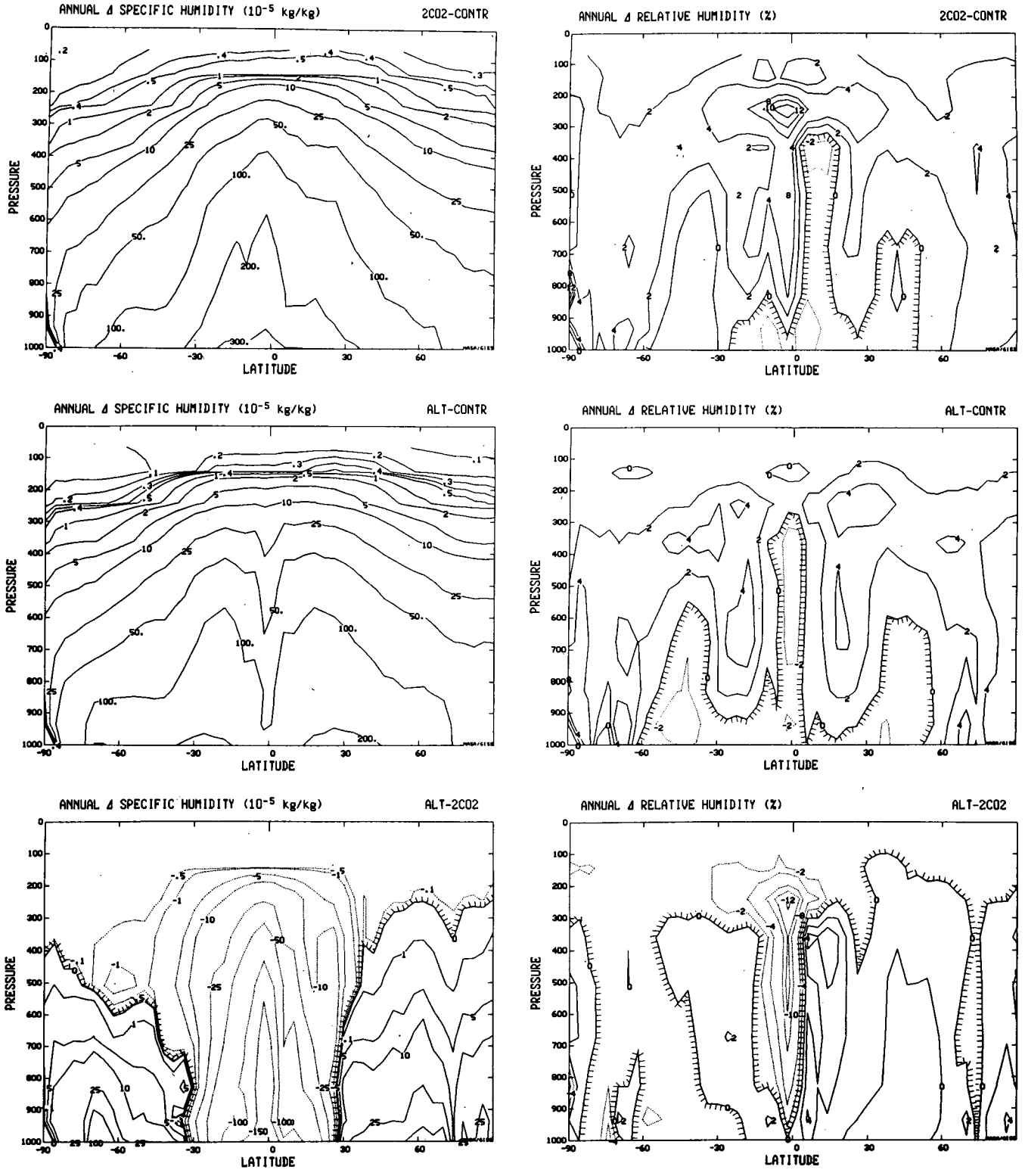

FIG. 5. Annual average change in specific humidity (left) and relative humidity (right), latitude versus pressure, for 2CO2 minus control, ALT minus control, and ALT minus 2CO2. Negative contours are dotted, and regions with negative changes are outlined with tic marks.

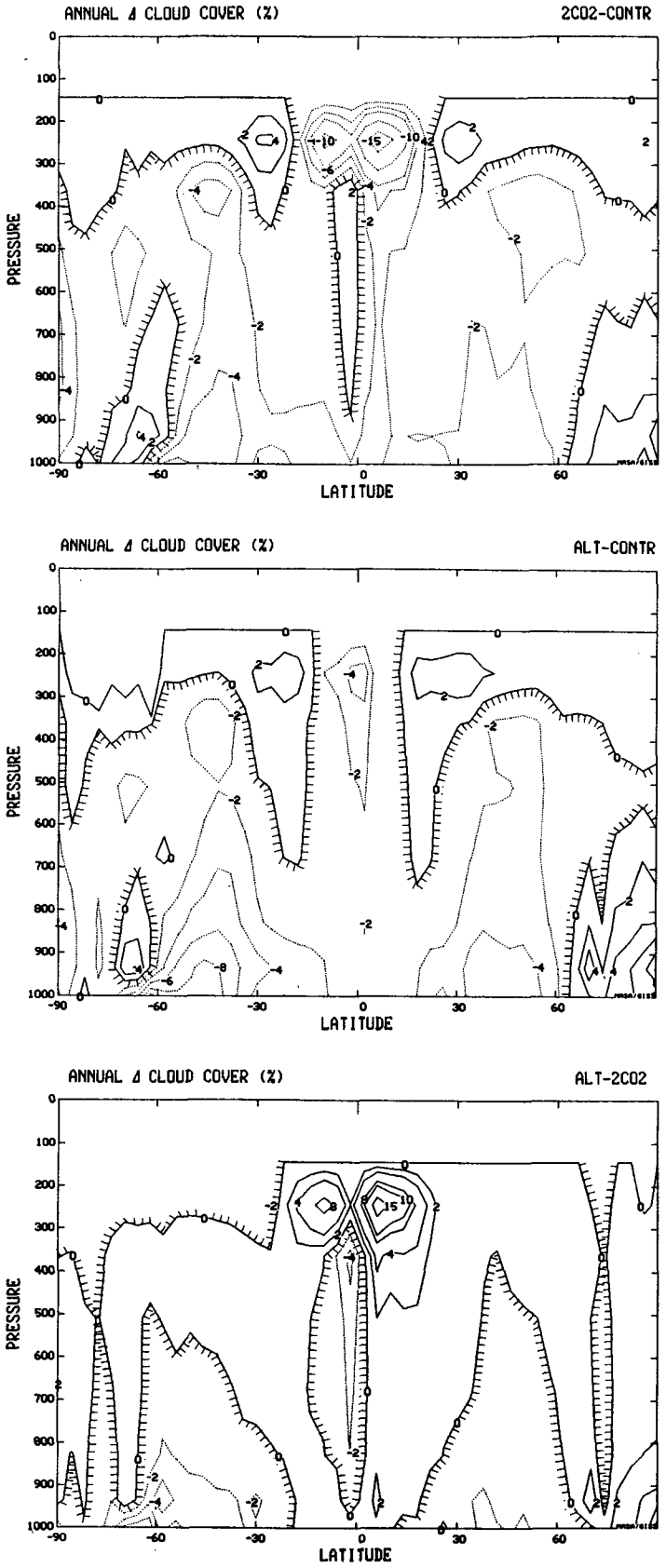

FIG. 6. As in Fig. 5, except for the annual average change in total cloud cover.

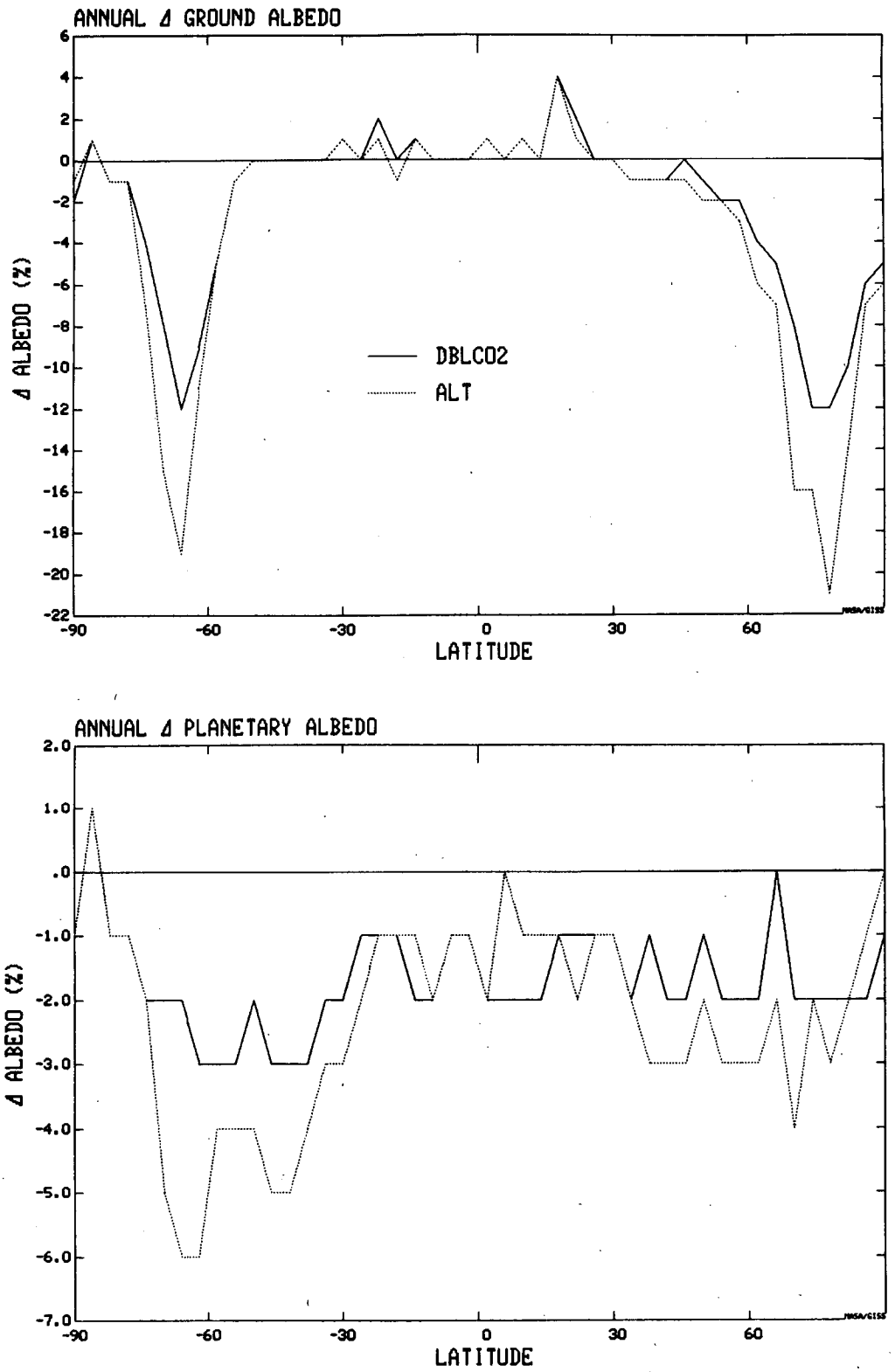

FIG. 7. Change in annual average ground albedo and planetary albedo, 2CO2 minus control (solid line), and ALT minus control (dotted line).

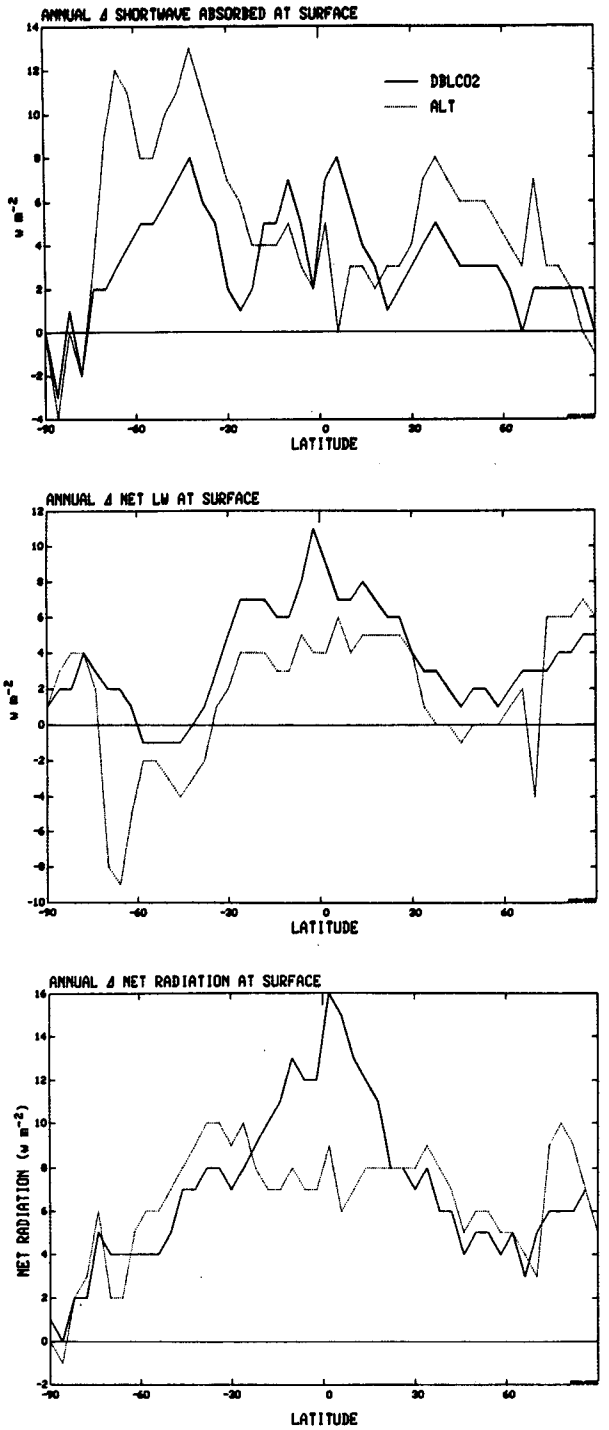

FIG. 8. As in Fig. 7, except for annual average change in shortwave radiation absorbed at the surface, net longwave radiation at the surface, and net radiation at the surface.

Hemisphere averages of relevant quantities vertically integrated throughout the atmosphere for December–February are presented in Table 2.

1) EVAPORATION AND PRECIPITATION

The impact of the differing sea surface temperature gradients on evaporation for the winter season is shown in Fig. 10. As noted above, in both experiments the tropical sea surface temperatures were higher than in the control run (Fig. 1), yet ALT shows an absolute decrease in low latitude evaporation. Similar changes occur in precipitation (Fig. 10). Although equatorial temperatures increased in ALT (by about 1.5°C), temperatures at other latitudes increase by more (e.g., 2.5°C at 14°N,S). This alters the sea surface temperature gradient, which then changes the low latitude circulation. In general, the warmest local sea surface temperatures help to initiate rising motion, and the meridional cell that is generated provides low level moisture convergence and latent heat release that amplify the initial ascent. In ALT, the changed meridional circulation produces subsidence over the equator, with somewhat higher sea level pressures and weaker winds; this then results in reduced evaporation. This type of result has occurred in various climate experiments (Rind, 1986, 1987). The change in evaporation depends sensitively on the exact sea surface temperature distributions in both the control run and experiment, which may be why the GFDL experiments do not show a minimum change in tropical evaporation.

The equatorial perturbations in evaporation and precipitation are replaced by perturbations of opposite sign or relative minima about 10°–20° latitude away (Fig. 10). This is also apparent in the vertical velocity changes (Fig. 11), with relative rising air initiated in 2CO2 where the sea surface temperature changes are most positive and the precipitation increase is largest. This scale for low latitude meridional cell changes is apparent in the precipitation differences generated by the other models for doubled CO_2 climates (Schlesinger and Mitchell, 1985, 1987) and in the GISS model simulations of Mesozoic and ice age climates (Rind, 1986, 1987). Since the scale is relatively similar in these different climates, it apparently does not depend on the details of the sea surface temperature distributions, but must be the result of some process that is similar in all of these climate experiments, such as the earth's rotation rate.

2) MEAN MERIDIONAL CIRCULATION

The altered sea surface temperature and precipitation distributions generate changes in the Hadley Cell streamfunction (Fig. 11), with increased magnitude away from the equatorial precipitation peak in 2CO2; the circulation changes produce relative subsidence over the equator in ALT. Again, changes of reverse sign are apparent 10°–20° latitude away. The influence of the thermal forcing on the Hadley Cell can be isolated by removing the eddy-induced streamfunction, leaving the transformed streamfunction (e.g., Dunkerton, 1978; Rind and Rossow, 1984). The transformed

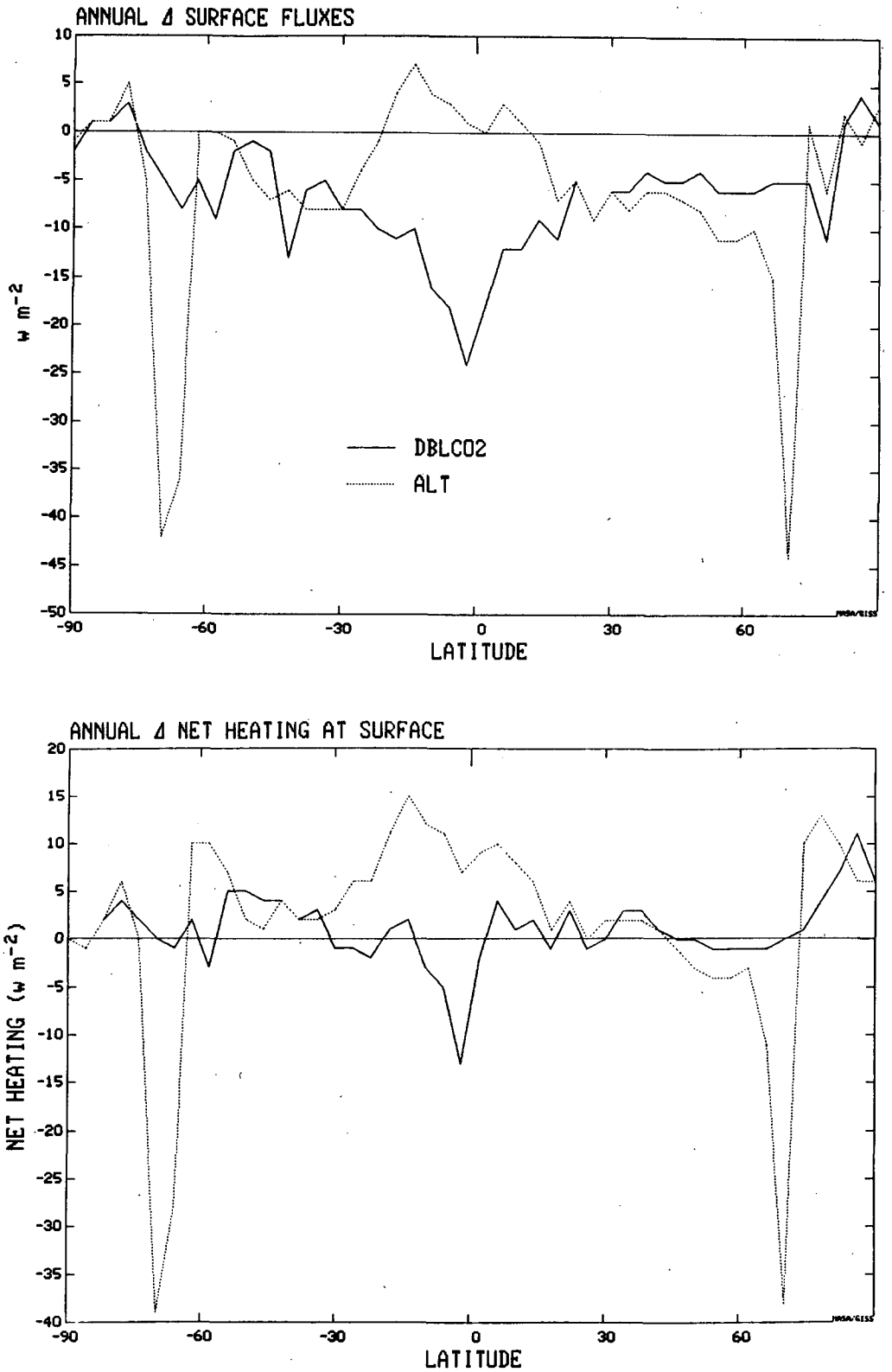

FIG. 9. As in Fig. 7, except for annual average change in surface fluxes (latent plus sensible heat) and net heating of the surface.

TABLE 2. Northern Hemisphere average results for December–February.

Climate variable	Control	2CO2	ALT
Evaporation (mm d^{-1})	3.51	3.87	3.75
Precipitation (mm d^{-1})	3.49	3.85	3.73
Hadley cell peak (10^9 Kg s^{-1})	−129	−135	−111
Hadley cell n'ward extent (°N.LAT)	37.5	38.8	38.8
Trans. s.f. tropical peak (10^9 Kg s^{-1})	−130	−140	−110
Trans. s.f. midlat peak (10^9 Kg s^{-1})	−230	−190	−180
Ferrel cell peak (10^9 Kg s^{-1})	32	29	29
Eddy–ind. s.f. midlat peak (10^9 Kg s^{-1})	240	200	190
Vert–int vert vel (10^{-5} mb s^{-1}) 2°N/26°N	17/−12	18/−11	11/−13
Zonal wind (m s^{-1}) 32°N, 200 mb	45.6	47.9	42.5
Stat eddy kinetic energy (10^4 J m^{-2})	22.8	20.5	23.4
Trans eddy kinetic energy (10^4 J m^{-2})	79.1	73.1	67.1
Eddy n'ward trans sens heat (10^{14} W)	17.1	15.2	14.9
Eddy n'ward trans latent heat (10^{14} W)	13.7	15.5	13.6
Eddy n'ward trans static energy (10^{14} W)	30.2	30.1	27.9
N'ward ep flux (10^{18} J)	−210.3	−208.1	−206.5
Vert ep flux (10^{18} J)	105.8	87.7	89.6
EP flux divergence (10^{18} J)	36.5	33.3	33.1
Atmos n'ward trans stat energy (10^{14} W)	45.1	47.9	42
Δ Sea surf temp (26°N–66°N)	19.3	19.8	18.2
Δ Vert–int air temp (26°N–66°N)	21.1	21.8	19.8

streamfunction change (Fig. 12) follows closely the change in latent heat release due to precipitation differences (Fig. 10) and is clearly responsible for the low and subtropical latitude Hadley Cell response.

The northward extent of the Hadley Cell shows a slight poleward shift in both of the experiments (Table 2), visible as the change to greater downward velocity poleward of 34°N. It results both from changes in the thermally induced streamfunction and from eddy effects. Precipitation is greater at higher latitudes in both experiments, and thus latent heat release produces a more thermally indirect streamfunction in each at midlatitudes (Fig. 12, transformed streamfunction). However, as shown below, reductions in eddy heat transports weaken the eddy-induced indirect Ferrel Cell (Fig. 12). The two processes are thus working in opposite directions and tend to minimize changes in the Hadley Cell poleward extent. A similar result was shown by Rind (1986, 1987) for the ice age and Mesozoic climate simulations. The small net weakening of the Ferrel Cell is consistent with the slight northward extension of the Hadley Cell (Rind and Rossow, 1984).

3) WIND FIELD

The two experiments show opposite influences on the jet stream, with the peak zonal wind values in the subtropics and lower midlatitudes increasing in 2CO2 and decreasing in ALT (Fig. 13, Table 2). This difference is understandable, via the thermal wind relationship, from the temperature change as a function of latitude in the two runs (Fig. 3). The jet stream is influenced by the mean circulation, including the Coriolis effect on the mean meridional wind, by eddy effects and by frictional processes, in this model due to the momentum mixing by convection. With the slight poleward extension of the Hadley Cell, the meridional wind at 200 mb and 32°N increased in both experiments by about 1.5×10^{-1} m s^{-1}, which when acted upon by the Coriolis force would increase the jet stream by about 32 m s^{-1} each month. The effect is minimized mainly by changes in the convergence of angular momentum due to the mean circulation itself, and, to a lesser extent, by increased frictional drag due to greater penetrating convection (Fig. 4). In addition, there are changes in the eddy forcing of the mean flow, as discussed below.

The geographic distribution of the 200 mb level wind change is shown in Fig. 14. In 2CO2 the increased subtropical jet stream across the southern United States and northern Africa is reminiscent of changes which have occurred in conjunction with El Niño events (e.g., Gray, 1984; Lau, 1985). The 2CO2 experiment resulted in substantial warming of the equatorial central and eastern Pacific (Hansen et al., 1984), where waters were relatively cool in the control run, similar to El Niño type changes. In ALT, even though sea surface temperatures are still warmer in this area of the Pacific relative to the control run, they warm more at other latitudes, and the jet stream weakens in the same areas it increased in 2CO2.

4) ENERGETICS

The energy diagram for the different runs is given in Fig. 15. The increased jet stream in 2CO2 is indicative of a small increase in zonal kinetic energy in that run. Although the warmer climate sea surface temperature distribution led to less generation of zonal available potential energy, in this run there is still relatively large transfer to zonal kinetic energy as a result of the equatorial Hadley Cell intensification. In addition, there is greater energy transfer from the eddies to the zonal mean flow, discussed below. In contrast, the zonal kinetic energy in ALT is less than in the control run, consistent with the decreased jet stream. ALT experiences greater decreases in the generation of zonal available potential energy, and in the zonal available potential energy itself, due to the sea surface temperature gradient in this run. The weaker Hadley Cell then results in less transfer from zonal available potential energy to zonal kinetic energy, and there is also less eddy forcing of the mean flow.

The control run and ALT both have relatively large amounts of generation of eddy available potential en-

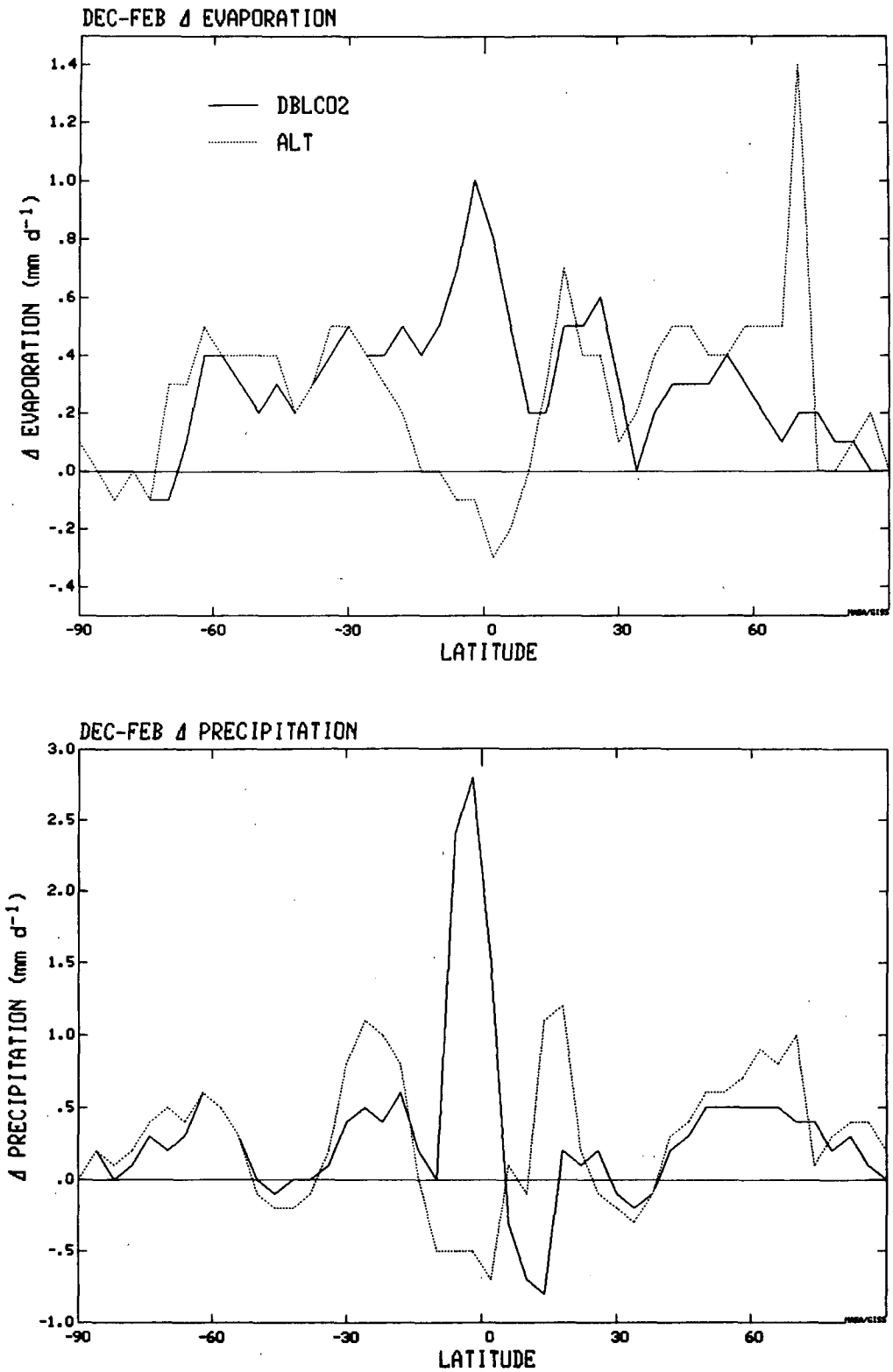

FIG. 10. Change in evaporation and precipitation from the three-year averages of December–February for 2CO2 minus control (solid line) and ALT minus control (dotted line).

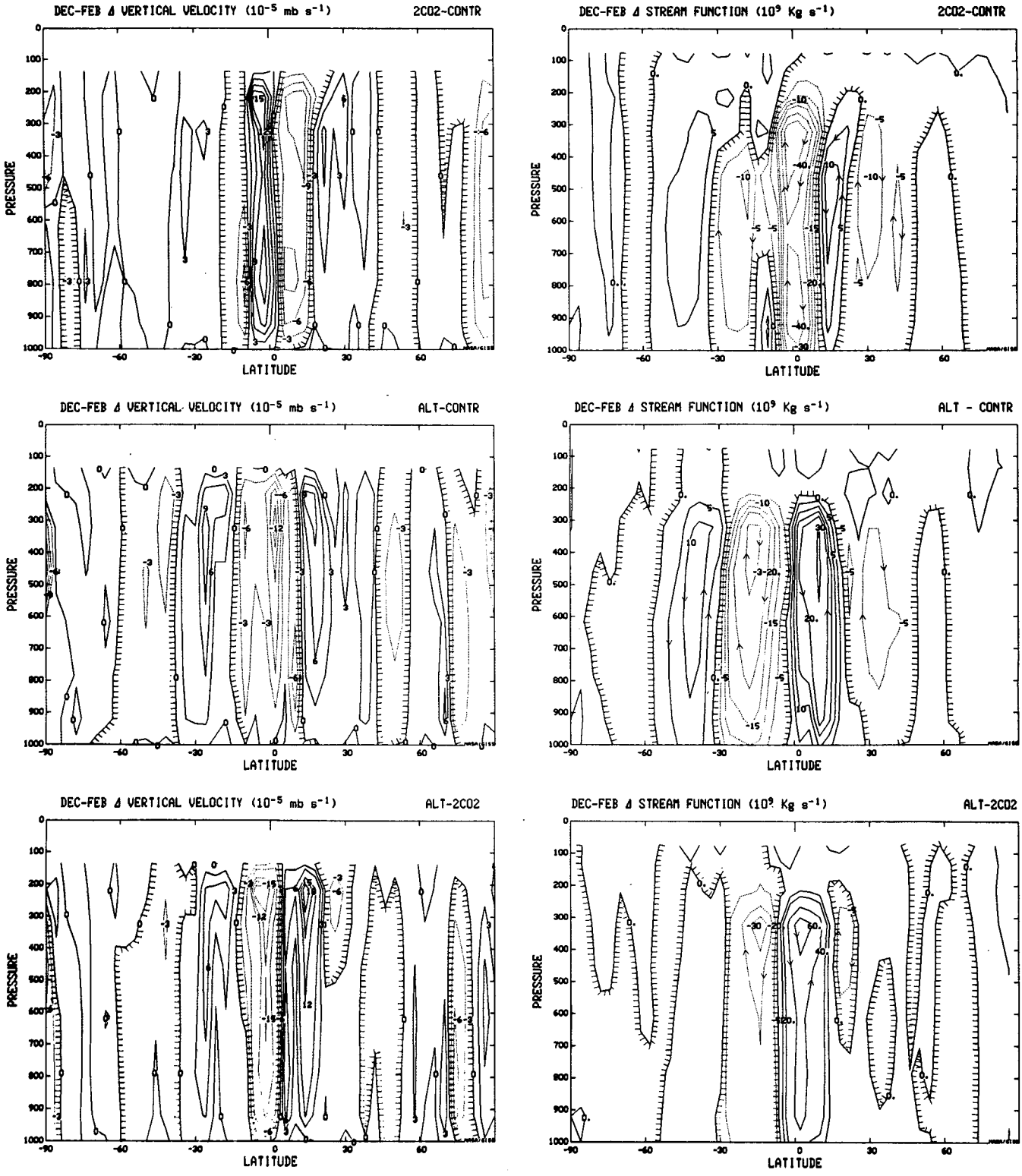

FIG. 11. Change in vertical velocity and streamfunction, latitude versus pressure, from the three-year averages of December–February for 2CO2 minus control, ALT minus control, and ALT minus 2CO2.

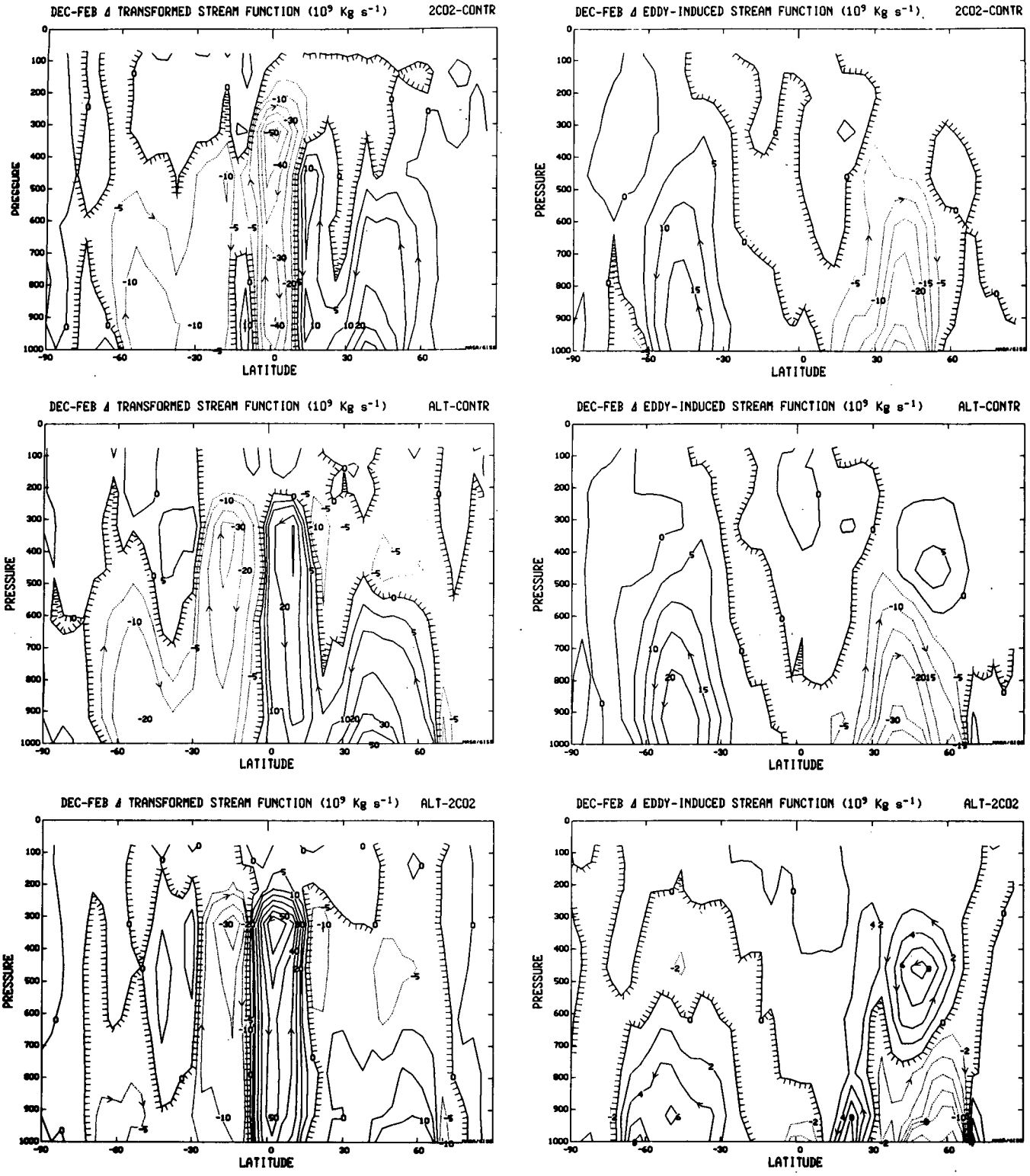

FIG. 12. As in Fig. 11, except for the transformed streamfunction and the eddy-induced streamfunction.

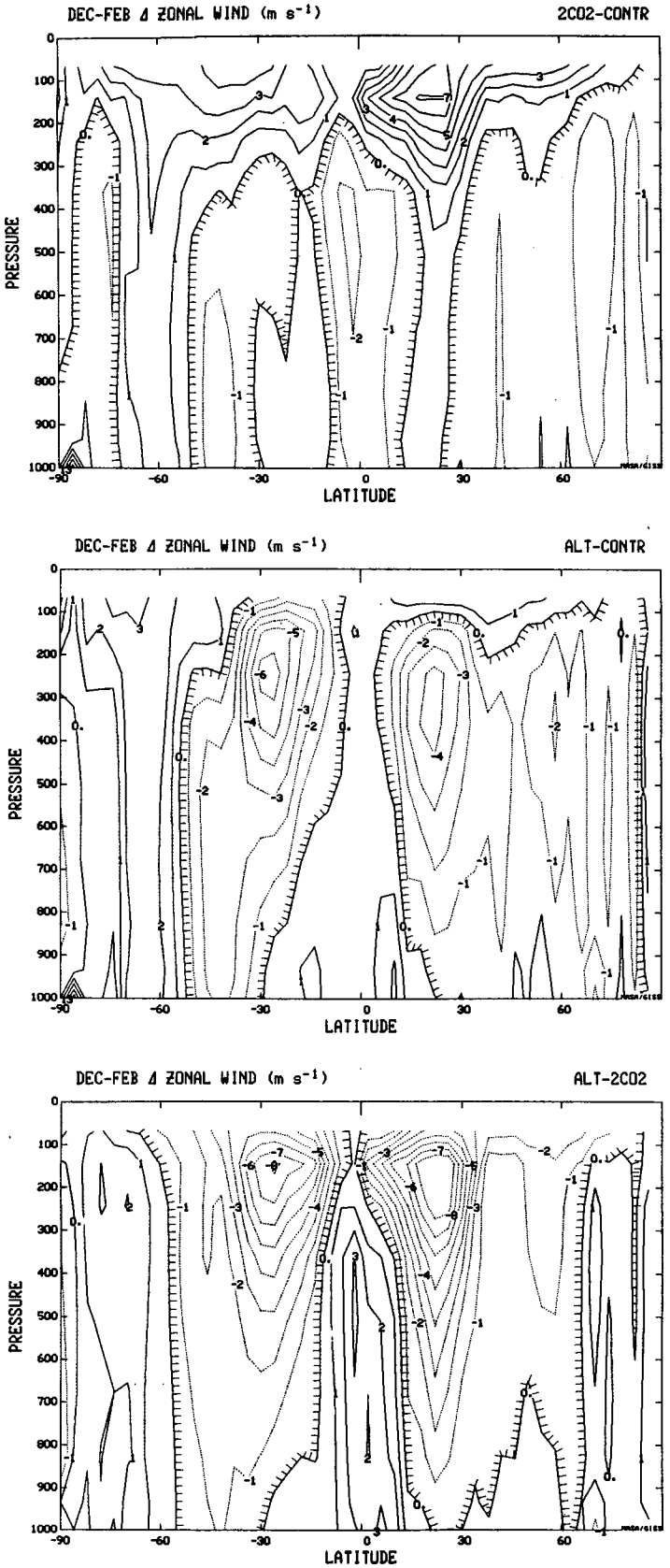

FIG. 13. As in Fig. 11, except for the zonal wind.

DEC-FEB Δ 200MB WIND

2CO2-CONTR

20 (M/S) REFERENCE

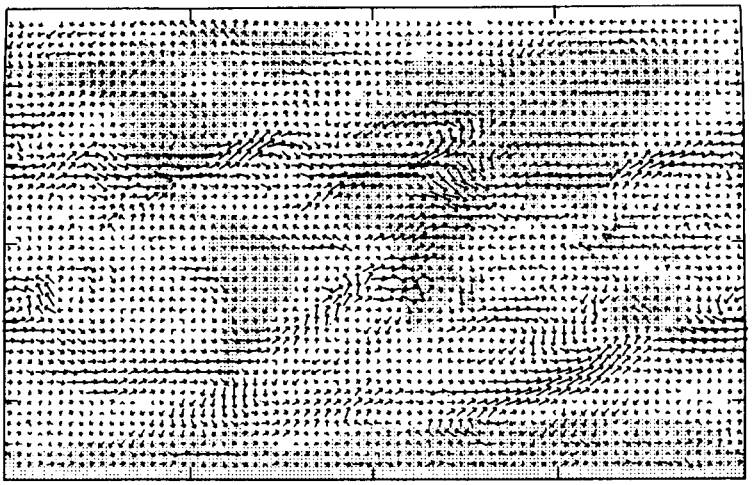

DEC-FEB Δ 200MB WIND

ALT-CONTR

20 (M/S) REFERENCE

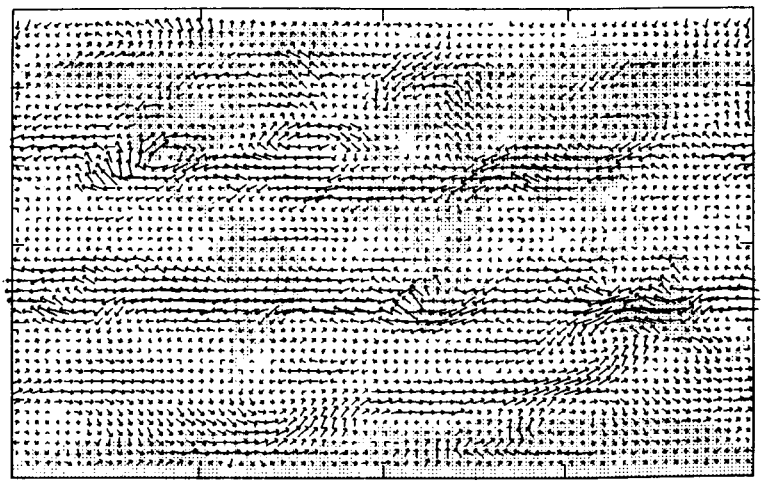

DEC-FEB Δ 200MB WIND

ALT - 2CO2

20 (M/S) REFERENCE

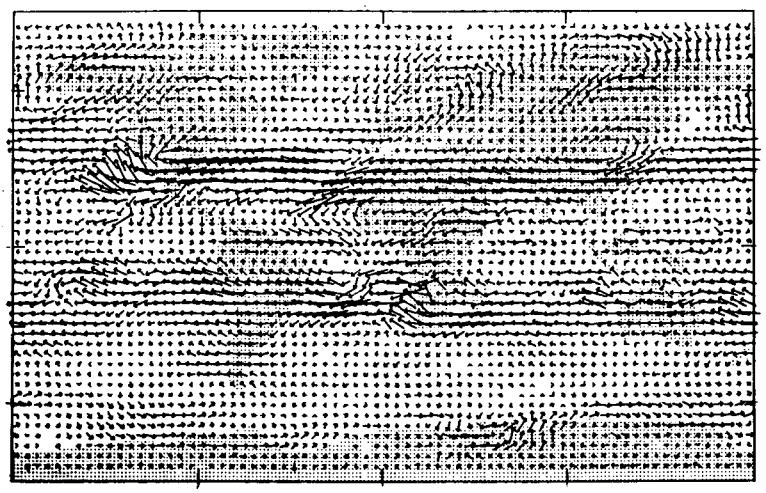

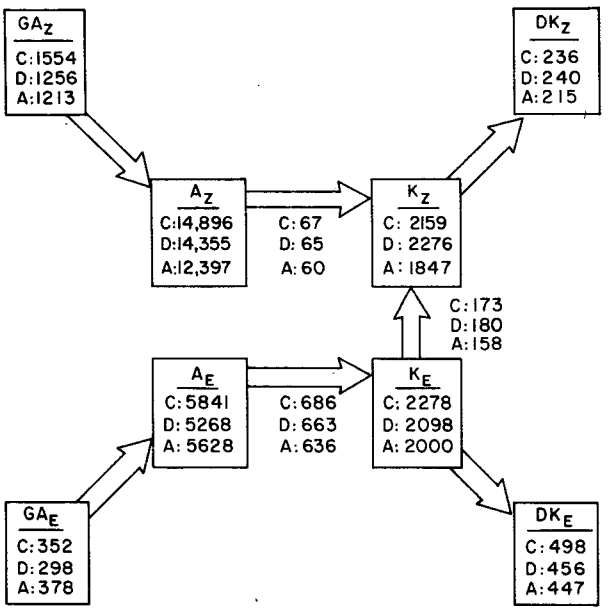

FIG. 15. Energy cycle diagram for the Northern Hemisphere troposphere from the three-year averages of December–February. Boxes represent zonal (Z) or eddy (E) available potential energy (A), kinetic energy (K), generation (G) or destruction (D), while arrows represent conversions between energy types (e.g., Saltzman, 1970). Units: 10^{17} J for energy, 10^{12} W for generation, destruction and conversions. Results are for the control run (C), 2CO2 (D) and ALT (A).

ergy and eddy available potential energy itself. This is due to the increased land–ocean temperature contrast in these runs in comparison with 2CO2, which has cooler midlatitude ocean temperatures than does ALT (Fig. 1). However, both of the experiments have reduced latitudinal temperature gradients and, as expected from quasi-geostrophic theory, reduced baroclinic energy conversions (more so in ALT). Eddy kinetic energy is thus largest in the control run.

The change in the vertically integrated eddy energy is shown in Fig. 16, along with the change in the standing and transient eddy components. Midlatitude decreases occur in both hemispheres in both experiments. The 2CO2 experiences a reduction in both the stationary and transient eddies, while in ALT reductions are predominantly in the transient component. As verified in the ice age simulations (Rind, 1987), the standing component depends upon the ocean–land contrast. The warm midlatitude ocean temperatures in ALT keep this contrast high, so stationary energy experiences little change. Transient eddy energy responds more to the latitudinal temperature gradient; as this gradient is reduced in both experiments, transient energy decreases in both, although the gradient change and the transient eddy decrease are greater in ALT.

The previous discussion can be elaborated by reference to the changes in the sea level pressure field (Fig. 17). If the sea level pressure is reduced in regions where it is normally low (e.g., the locations of the Icelandic and Aleutian Lows), the stationary eddy energy will increase. In 2CO2 the resulting sea surface temperature distribution and land–ocean temperature contrast produced higher pressures over the North Atlantic and Pacific, and stationary energy decreased. In ALT the very warm northern ocean waters kept the sea level pressures low in these regions, and stationary eddy energy was less affected. With a reduction in the latitudinal temperature gradient, baroclinicity was reduced, and transient energy diminished.

Due to the influence of the sea surface temperature distribution on the oceanic pressure field, 2CO2 experienced decreases in stationary longwave energy for wavenumber 1, while ALT did not (Fig. 18), which would have implications for changes in stratospheric dynamics. In general, though, the decreased latitudinal temperature gradient resulted in weaker longwave energy, as expected from studies of baroclinic instability (e.g., Green, 1960).

5) ENERGY TRANSPORTS

The reduced eddy energy results in reduced eddy transport of sensible heat, but, with increased moisture in the atmosphere, eddy latent heat transport increases in both experiments (Fig. 19). The moist static energy transport shows little change in 2CO2, with the reduced eddy energy balanced by the increased moisture availability. In ALT the reduction in eddy energy and sensible heat transport is large enough, and the increase in specific humidity small enough, to diminish the total eddy energy transport. This difference in eddy moist static energy transport also arose when comparing the modeled doubled CO_2 climate with warm equatorial sea surface temperatures (as in 2CO2) and the Mesozoic climate with relatively cool equatorial waters (Rind, 1986).

The effect of the change in eddy energy and eddy transports on the mean circulation can be described in terms of the Eliassen–Palm (EP) flux (Eliassen and Palm, 1961; Andrews and McIntyre, 1976). The meridional and vertical components of the Eliassen–Palm flux represent the wave energy flux normalized by the zonal wind. In the control run, wave energy is generated in midlatitudes at low levels and propagates vertically away from the surface, toward both low and high lat-

FIG. 14. Change in 200 mb wind, latitude versus longitude, from the three-year averages of December–February for 2CO2 minus control, ALT minus control, and ALT minus 2CO2. Tic marks show latitudes of 0°, ±30°, ±60° and longitudes of 90°W, 0° and 90°E.

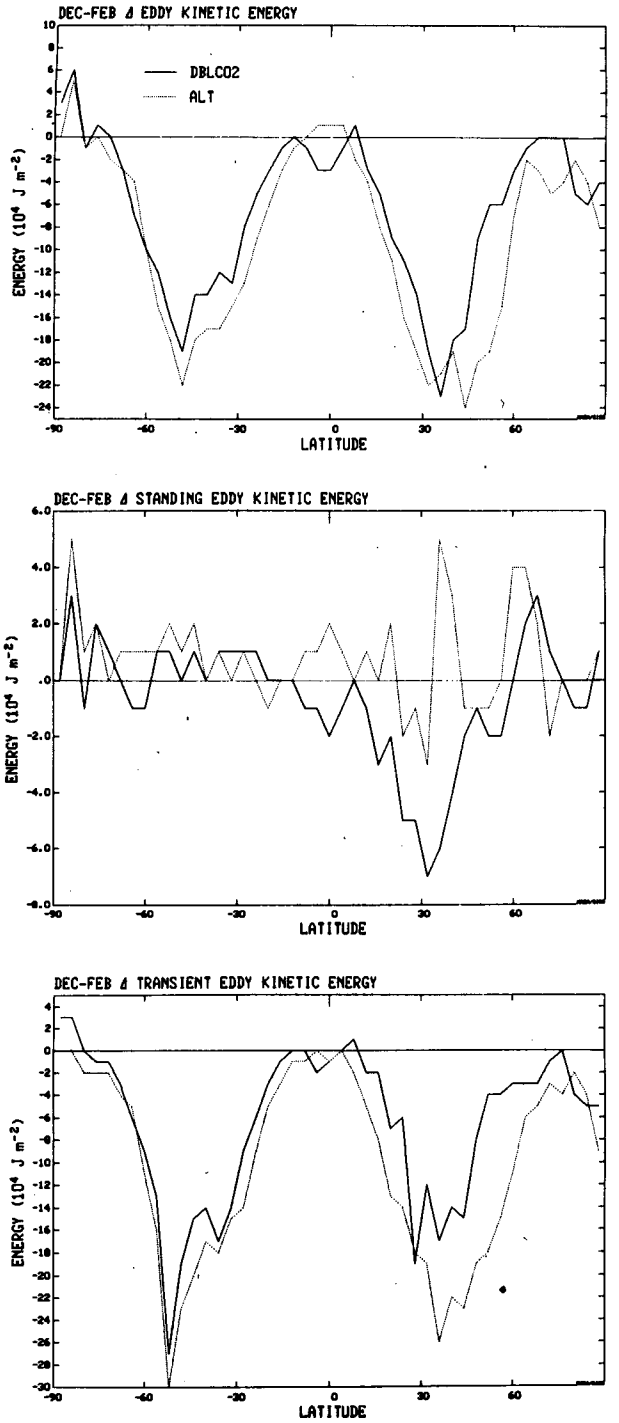

FIG. 16. As in Fig. 10, except for eddy kinetic energy, standing eddy kinetic energy, and transient eddy kinetic energy.

itudes (Fig. 20). The energy converges at the tropical upper troposphere zero wind line separating low latitude east winds from midlatitude west winds, a critical level for stationary waves (which dominate the monthly average EP flux divergence). This convergence provides an easterly acceleration to the winds, drawing the zero wind line farther north into the winter hemisphere. The control run pattern of EP flux divergence (Fig. 20) resembles the observed pattern, as well as that of the complete life cycle for baroclinic instability (Edmon et al., 1980).

In both 2CO2 and ALT there is reduced wave energy generation due to the reduction in the latitudinal temperature gradient. This produces decreases in the ver-

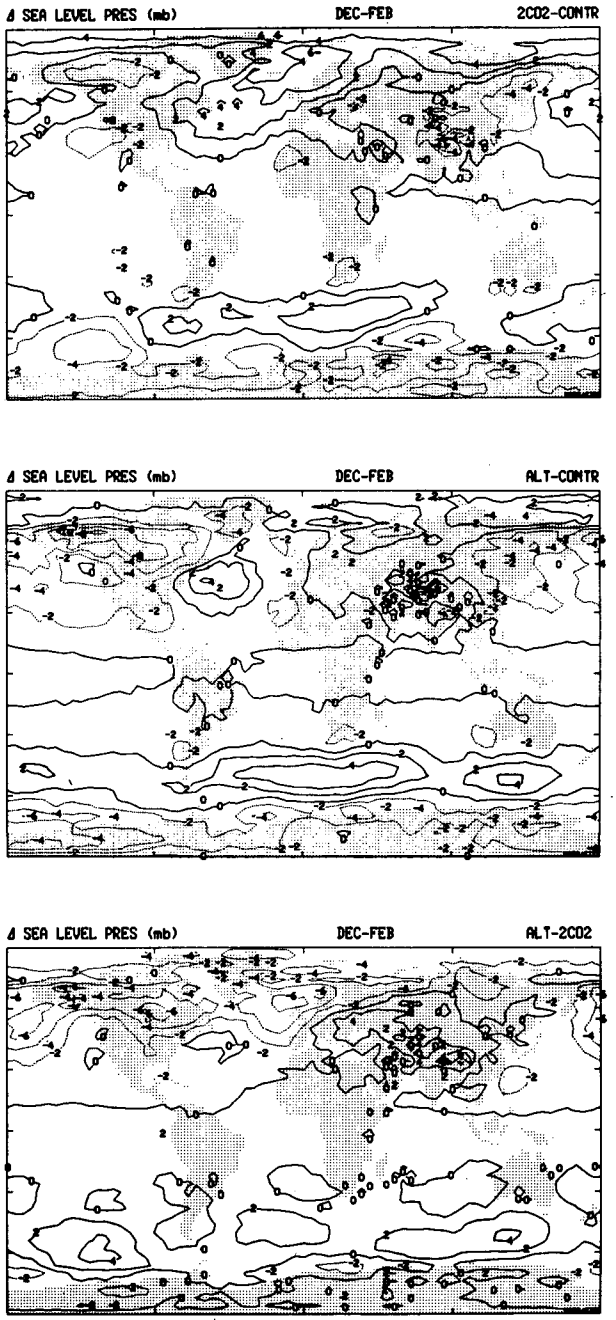

FIG. 17. As in Fig. 14, except for sea level pressure.

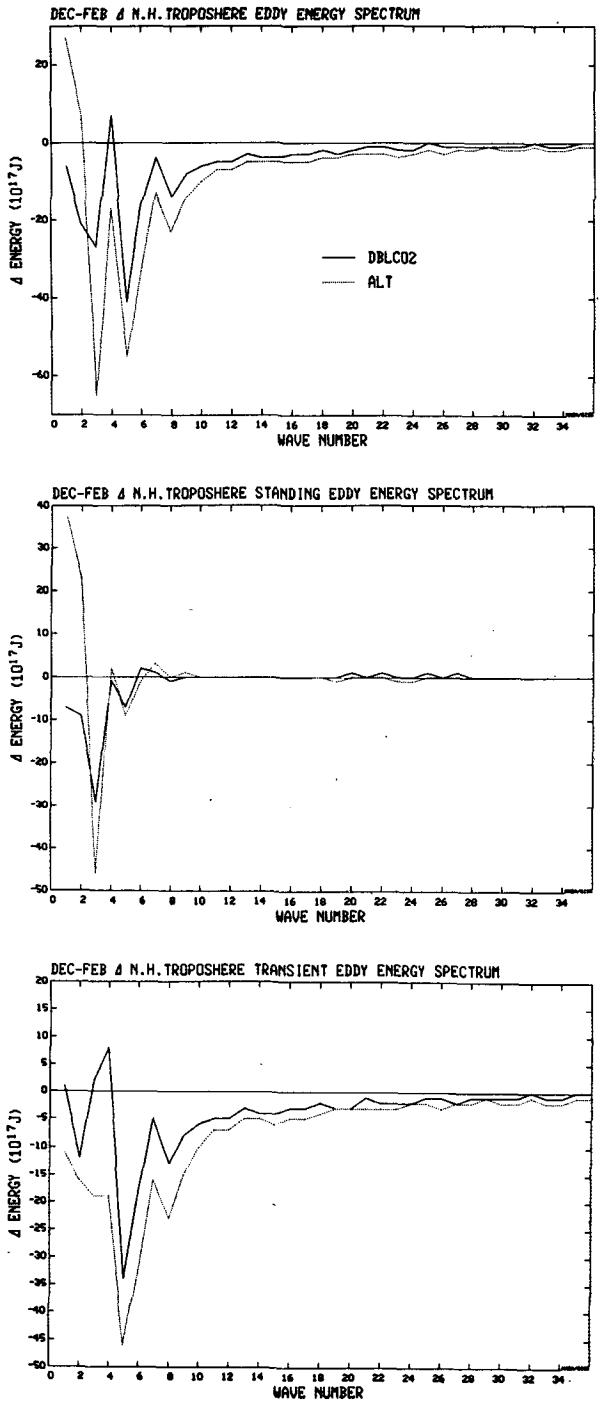

FIG. 18. Change in the energy spectrum from three-year averages of December–February for total eddy energy, standing eddy energy, and transient eddy energy. 2CO2 minus control (solid line), ALT minus control (dotted line).

tical and meridional wave energy fluxes that existed in the control run (Fig. 21). The changes in the two experiments are slightly different, as the eddy energy and proportion of transient to stationary eddy energy differ. The effect in both, however, is to decrease the EP flux convergence or divergence occurring in the control run (Fig. 20). In particular, this means there is less of a tendency for the eddies to decrease the subtropical upper troposphere zonal wind; comparison of the change in EP flux divergence with the zonal wind change (Fig.

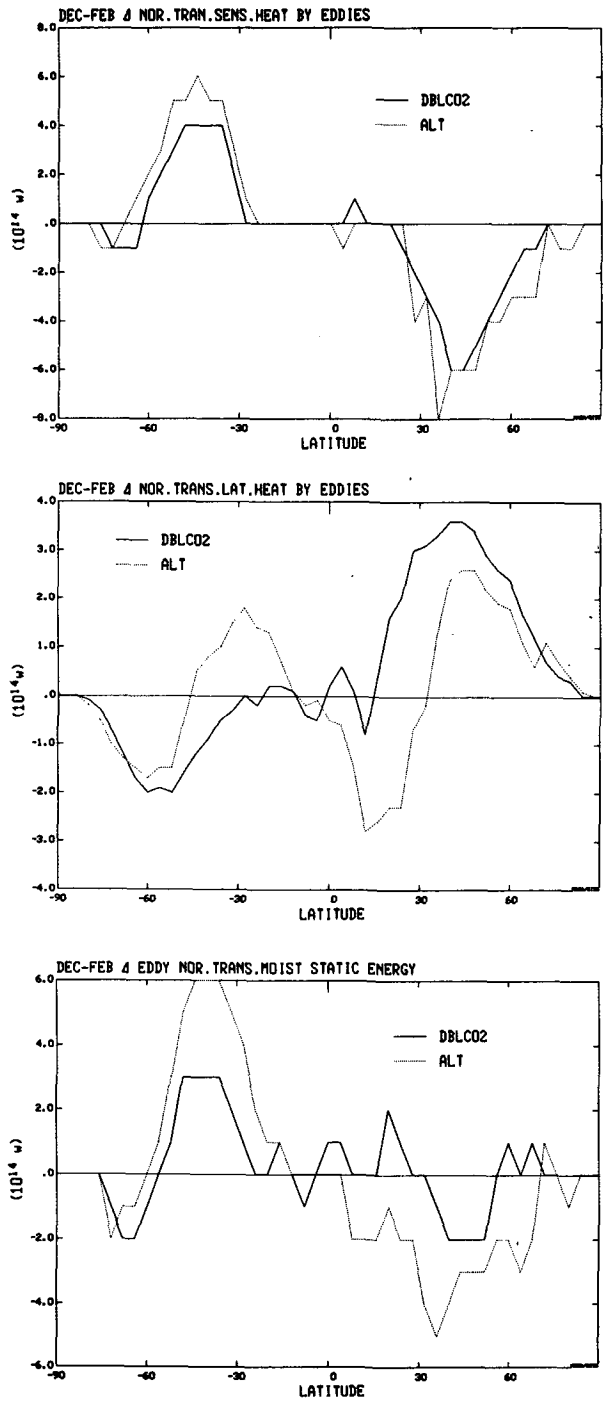

FIG. 19. As in Fig. 10, except for eddy northward transport of sensible heat, latent heat, and static energy.

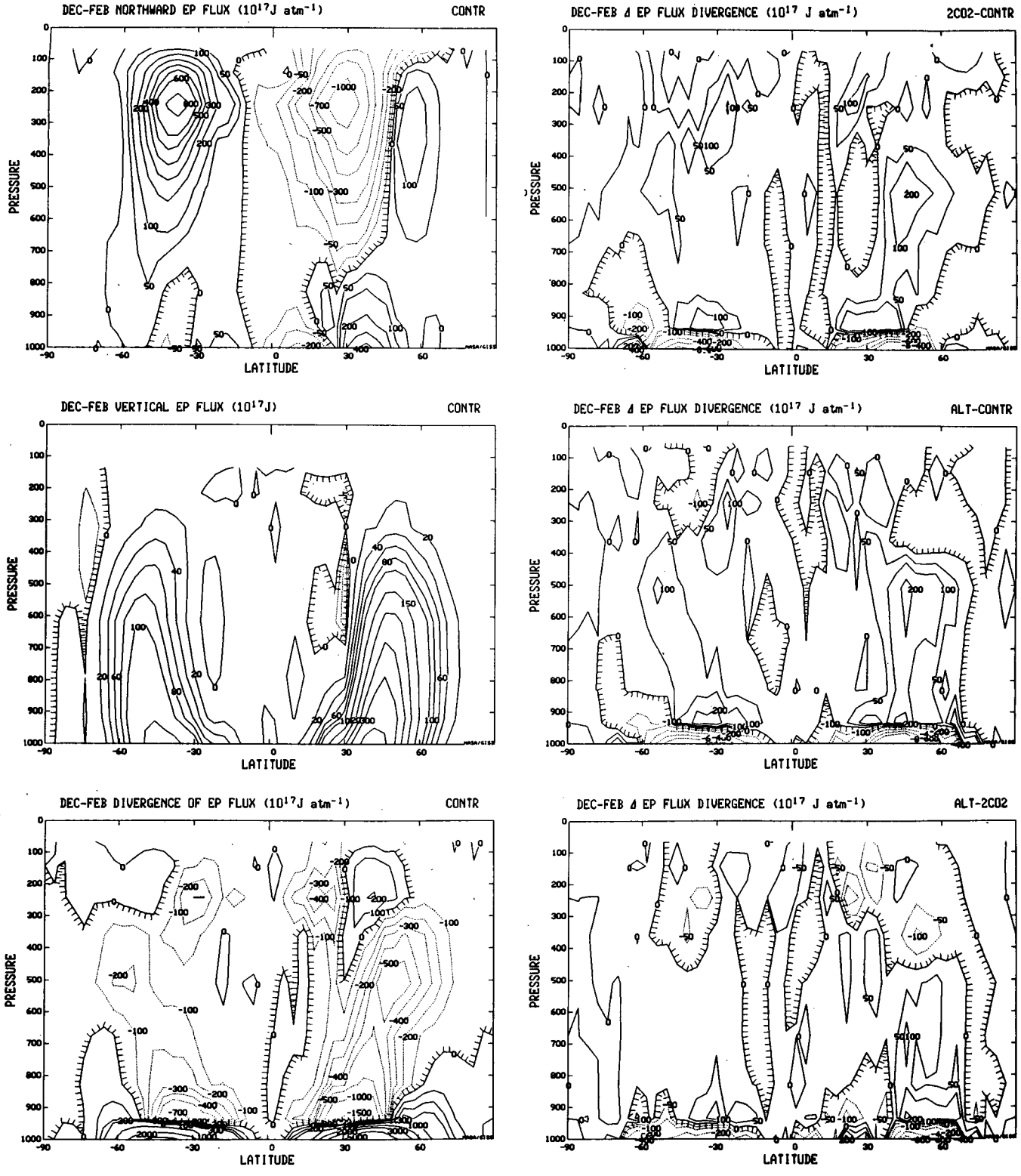

FIG. 20. Three-year averages of December–February control run EP flux values (left) and change in EP flux divergences for 2CO2 minus control, ALT minus control, and ALT minus 2CO2.

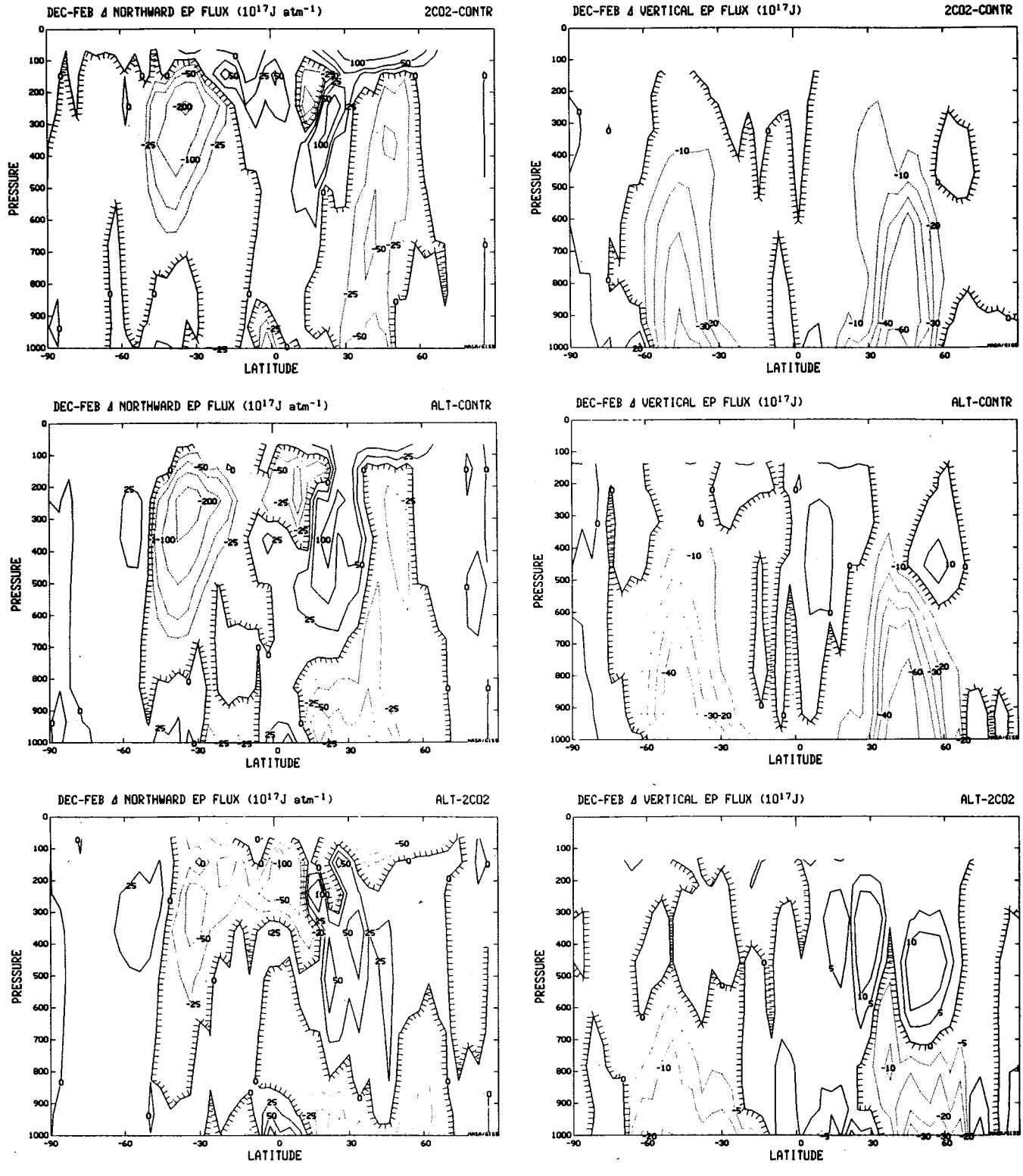

FIG. 21. As in Fig. 11, except for northward EP flux and vertical EP flux.

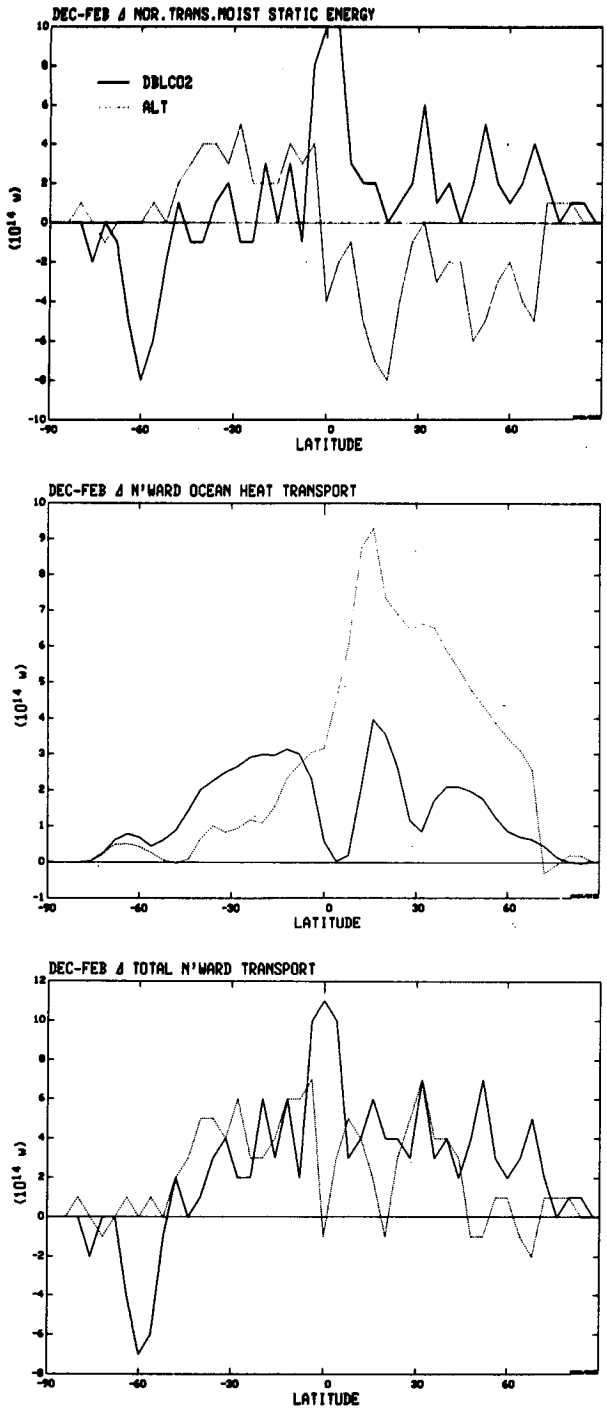

FIG. 22. As in Fig. 10, except for northward transport of static energy by the atmosphere, implied northward transport of heat in the ocean, and total (atmosphere plus ocean) northward transport of energy.

13) indicates that the increased subtropical jet stream in 2CO2 is accompanied by a relative increase in EP flux divergence, with a magnitude that would augment the zonal wind speed at 200 mb and 28°N by 15 m s^{-1} each month. As noted above, ALT experiences little change in stationary eddy energy (Fig. 16), and the change in the monthly mean EP flux divergence is less. Thus, the change in eddy energy is doing less to accelerate the jet stream in this run, and the jet stream decelerates due to other processes (mean cell effects responding to the decreased temperature gradient, from the thermal wind relationship). The differences in eddy forcing of the jet stream between these experiments and the control run is consistent with the change in energy transfer from eddies to the mean flow for the hemispheric average (Fig. 15).

The change in total atmospheric energy transport is presented in Fig. 22. Here 2CO2 shows increased poleward energy transport in both hemispheres, while ALT shows decreases. These changes are consistent with the change in the vertically integrated air temperature gradient and also the ice-free sea surface temperature gradient across midlatitudes (Table 2), two gradients which appear to be closely connected and apparently help govern the total atmospheric transport (Rind, 1986). The energy transport difference is due primarily to the change in latent heat transport, increasing in 2CO2 with its warm tropical sea surface temperatures and relatively large eddy energy, and decreasing in ALT due to the opposite tendencies. The result in ALT is similar to that obtained by Manabe and Wetherald (1980) for doubled CO_2, as might be expected considering that the imposed sea surface temperature gradient in ALT is qualitatively similar to that of the GFDL experiments.

Large implicit ocean heat transports were required to produce the warm high latitude ocean temperatures in ALT. We can determine the magnitude of transport needed by calculating the net heat convergence needed to compensate for the surface energy fluxes and the deviation of the model from exact energy balance. To estimate this result for a particular season we proceed as in Rind (1986) by assuming that the net heat storage is proportional to the magnitude of the needed convergence. The result shown in Fig. 22 indicates the large ocean heat flux assumed in this run, warming higher latitudes and cooling the tropical ocean. If the climate changes in the fine grid model used for this experiment were exactly similar to those in the coarse grid runs (from which the specified doubled CO_2 sea surface temperatures for 2CO2 were obtained), there would be no implied ocean heat transport for 2CO2. The deviations from zero shown for 2CO2 in Fig. 22 are indicative of the difference between the two models; the fine grid control and 2CO2 runs have less cloud cover, lower planetary albedo, and thus more energy received at the surface, but also more evaporation due to stronger low latitude winds, resulting in patterns of needed increases and decreases of heat convergence.

The total energy transport change in the two experiments, the sum of the oceanic and atmospheric transports, is presented in Fig. 22. With little implied ocean

heat transport change, 2CO2 produces larger total transports due to the atmospheric changes discussed above. The large ocean heat transports in ALT more than compensate for the diminished atmospheric response. In both runs the total system dynamics is providing a positive feedback to the change in the surface air temperature latitudinal gradient, contrary to the assumption used in energy balance models, as the poleward atmospheric plus oceanic energy transports increase despite the reduced latitudinal temperature gradient.

c. *Regional changes*

How dependent are the regional changes forecast for the doubled CO_2 climate on the sea surface temperature gradient changes? Manabe and Wetherald (1986), using a model with predicted cloud cover, reported reductions in summertime soil moisture over much of the extratropical Northern Hemisphere land regions. This result was similar to their earlier findings with fixed cloud cover (e.g., Manabe et al., 1981) and led them to conclude that it was not qualitatively dependent upon the cloud cover changes. The reasons for the decrease in summertime moisture in their model are a combination of changes in evaporation, precipitation and snow melt. Since the findings discussed above indicate that both the thermal and hydrologic balances vary with the sea surface temperature gradient, it is of interest to see how the differences in these gradients influence soil moisture values and regional climates.

The regional distribution of the Northern Hemisphere summertime (June–August) surface air temperature change is presented in Table 3. There is a general summertime warming over land, more so in ALT at midlatitudes and less in ALT at lower latitudes due to the sea surface temperature change distribution (Fig. 1). The effect of the warming at different latitudes on the spring and fall temperatures can be gaged by examining the change in the growing season (consecutive days with temperatures above freezing) in these experiments (Fig. 23). (Note that these values have not been derived from model simulations in equilibrium, due to the specification of the sea surface temperatures.) At midlatitudes ALT has a much longer growing season, due partly to a decrease in late frosts (thus resulting in earlier spring snowmelts).

Temperature differences in individual regions arise from changes in the local atmospheric circulation. The 2CO2 has cooler sea surface temperatures at midlatitudes than does ALT, and so has higher sea level pressure over the North Atlantic and the eastern Pacific. This pressure pattern produces more onshore flow and reduces the warming in certain regions, such as western Europe and the eastern United States. Similarly, higher pressures in ALT equatorward of 30° latitude provide for a greater southwesterly flow to lower midlatitudes and extend the influence of the reduced subtropical warming to southern portions of Eurasia and North America.

The change in precipitation (Fig. 24) is dominated by the low latitude influence of the sea surface temperature gradients, with equatorial increases in 2CO2 and decreases in ALT. The reverse occurs in bordering regions. Midlatitude changes tend to be smaller in magnitude, with the major effect being the increased rainfall in the southern portions of continents in ALT, as the increased southwesterly flow extends the increased monsoon subtropical rains northward. As indicated in Table 3, there is much variability in the rainfall changes for the different experiments from region to region, and assessments for altered precipitation due to doubling of CO_2 would be very different in places such as the African Sahel, Indian Desert or southern China, depending upon which sea surface temperature gradient prevailed.

The change in evaporation, precipitation minus evaporation (P − E), and soil moisture for the different regions is listed in Table 3, and the soil moisture change results for the last summer are given in Fig. 25. Evaporation increases in most cases due to the warmer summer temperatures, and thus more so in ALT in most mid- and high latitude regions. P − E changes vary from region to region; in many midlatitude locations it is dominated by the evaporation change. The resulting summer soil moisture differences integrate this effect with changes in runoff and springtime soil moisture. There are large soil moisture differences in the tropics and subtropics, with changes of different sign in many regions, as was true for precipitation. At other latitudes there are some qualitative similarities in the patterns of soil moisture change in the two experiments, such as moistening over Scandinavia, drying at most other high latitude locations, moistening in southern Canada, and drying in the eastern United States. However, even in these areas there are often quantitative differences; the central and eastern United States are considerably drier in ALT with its warmer temperatures (Table 3), a result more similar to that of Manabe and Wetherald (1986). ALT is wetter through most of the subtropics and in regions such as northern Russia, in contrast to the GFDL result, and neither run indicates the relatively complete drying of extratropical land masses shown by Manabe and Wetherald (1986). (Note that there has been no attempt to make the sea surface temperature changes in ALT precisely equal to those of the latest GFDL doubled CO_2 experiment.) These results emphasize that uncertainties in the climate system/ocean response, and in the appropriate sea surface temperature gradient, induce large uncertainties into the forecast of soil moisture changes.

To illustrate how the different dynamical changes in the two experiments influence the regional climate simulations, we summarize the seasonal average change in the synoptic pattern over North America. A sche-

TABLE 3. Regional climate

Change Exp-Cont		West U.S.	Mid U.S.	East U.S.	South Cnda	Grnland	Mid Eur.	Nor. Russ	West Sibr	Sibr plat	South Chna
Surf temp (°C)	2CO2	5.3	5.4	4.8	5.2	2.9	2.8	3	5.3	3.7	3.4
	ALT	4.9	6.2	6.1	4.5	3.2	4	3.1	4.9	3.6	4
Prec (mm d^{-1})	2CO2	−0.1	−0.4	0.2	−0.3	1	0.1	0.8	0	0.4	0.8
	ALT	0.2	−0.2	0.3	0.3	0.5	−0.1	1.5	0.5	0.4	−0.9
Evap (mn d^{-1})	2CO2	0.2	−0.2	0	0.2	−0.2	0.4	0.7	0.2	0.4	0.3
	ALT	0.4	0.5	−0.2	0.5	−0.1	0.6	1.2	0.4	0.4	−0.2
P − E (mm d^{-1})	2CO2	−0.3	−0.2	0.2	−0.5	1.2	−0.3	0.1	−0.2	0	0.5
	ALT	−0.2	−0.7	0.5	−0.2	0.6	−0.7	0.3	0.1	0	−0.7
Soil moist (kg m^{-2})	2CO2	5.3	−4.5	−16.9	−18.9	−0.6	6.4	43.8	−17	−23.7	1.9
	ALT	9.7	−11.1	−24.4	8.1	−1.7	−9.6	83.4	0.7	−21.4	−54

matic of the precipitation and jet stream level wind changes is presented in Fig. 26. As discussed above, the dynamical changes result from differences in the latitudinal temperature gradient and the land–ocean contrast.

In winter, 2CO2 features greater ridging over the northeastern United States with troughing in the west (at 500 mb). ALT experiences ridging over the northeastern United States and additional ridging in northwestern Canada, while troughing occurs farther west, off the west coast. The increased subtropical jet stream in 2CO2 moves weather systems along the southern border; in conjunction with the western trough, this provides for more rain in the southwest. Storms then track due east through the Gulf of Mexico. In ALT, as noted earlier, the jet stream decreases; in particular, the subtropical jet is less effective in bringing storms northeastward through the eastern half of the country, and the jet stream turns northward, steering storms through the mountain states and then along the Canadian border. The runs thus do show differences in the winter precipitation patterns, although various similarities exist.

This combination of similarities and differences also exists in other seasons. In spring, both runs experience ridging in the east, although the effect is much stronger in ALT, and troughing in the west. In summer, 2CO2 has ridging in the west and troughing in the east; the effect is more muted in ALT. In fall, both runs develop ridges over the central United States, but 2CO2 develops a trough over the east coast, while ALT has troughs in the extreme west and south. Precipitation change patterns are similar to the same extent that the long-wave patterns are, with some regions of agreement. Both runs get more rain over Canada, but the effect is greater in ALT with its warmer temperatures. The subtropical jet stream decreases in ALT and increases in 2CO2; apparently, the change in the long-wave and medium-wave pattern at midlatitudes, relatively similar in the two runs, is not highly dependent on the completely dissimilar change in the subtropical jet stream magnitude. Note that for the hemisphere as a whole, while the two experiments experience different magnitudes of decrease in their standing and transient eddy energies, the wavenumber response patterns are generally similar (Fig. 18). In all seasons the surface air temperature warms more in ALT, by 1°–2°C, which provides for greater evaporation, snow melt and soil moisture changes. Water availability would thus be different in the two climates, as indicated in Table 3, even when precipitation changes are similar.

Another major concern associated with climate warming is the fate of high latitude land ice and, thus, sea level (e.g., Barth and Titus, 1984; Meier, 1985). Warming should accelerate ice melting, but might also lead to additional precipitation, which could increase snow cover. Both doubled CO_2 experiments show these effects, but they are larger in ALT as a result of its warmer high latitude sea surface temperatures. The change in the components of the hydrologic cycle over Greenland and Antarctica are presented in Table 4. Annual precipitation and runoff increase as climate warms, while evaporation shows little change. In the model, ice elevation is kept constant, and thus, when runoff plus evaporation exceed precipitation, ice "emerges" to maintain constant elevation. In this fashion the model keeps track of ice melting, and, as indicated in Table 4, ice melting occurs in both experiments except at the very highest latitudes in Antarctica. Since the land ice model is very crude, the calculated ice melting values cannot be used to imply sea level rise; nevertheless, the results do indicate that potential ice sheet changes are amplified in ALT.

4. Discussion and conclusions

a. Energy balance

The radiation balance results clearly show the feedbacks that help generate, or are consistent with, the strong low latitude warming found by the GISS model in its doubled CO_2 equilibrium run. With warmer equatorial sea surface temperatures as in 2CO2, upper level clouds decrease and allow more shortwave radiation to be absorbed at the surface. In addition, the at-

changes (June–August).

Chna dsrt	Ind. dsrt	Aus. dsrt	North Shra	South Shra	Afr. Sahl	Afr. rain	Amzn rain	North Atl.	Mid Atl.	North Pac.	West Pac.	East Pac.
2.8	4.5	4.9	5.1	4.6	4.6	4.3	4.9	3.6	3.3	4.2	3.8	4.1
4.1	2.9	4.9	3.6	1.1	1.9	2.1	2.3	4.6	2.8	5.1	2.1	1.8
1.9	0.7	0.2	0.2	0.2	0.3	1.4	−0.2	0	0.1	0	0.9	1.1
1	2.1	−0.1	0.7	1.9	1.4	0.5	0.4	0.3	0.1	−0.2	−0.1	−0.2
0.9	0.5	0.1	0.2	0.3	0.4	0.4	0.2	0	0.3	0	0.5	0.4
0.6	0.7	−0.1	0.6	1.4	0.6	0.3	0.4	0.2	−0.3	0.2	0	−0.1
1	0.2	0.1	0	−0.1	−0.1	1	−0.4	0	−0.2	0	0.4	0.7
0.5	1.4	0	0.1	0.5	0.8	0.2	0	0.1	0.4	−0.4	−0.1	−0.1
18.4	8.2	1.1	0.1	−1.1	−19	30.5	−44.1	—	—	—	—	—
11.4	22.3	−1.2	0.4	4.4	21.2	7.7	−1.1	—	—	—	—	—

mospheric specific humidity increases, producing more net longwave radiation at the surface. The total net radiation absorbed at the surface is thus much higher and would help produce warmer sea surface temperatures. In ALT, and possibly in the GFDL climate simulations, both cloud cover and moisture changes are considerably diminished and are consistent with the reduced warming of the tropical ocean temperatures. While the mechanisms are thus understandable, these results cannot indicate why the different GCMs get into the different cycles in the first place. The particulars of the GISS cloud generation scheme, discussed above, or the GISS penetrative convection scheme, may be important in this regard.

Although ALT has much less radiation at the surface than 2CO2, it has more net heating, because the evaporative energy loss in ALT is relatively small. So ALT has an implicit equatorial ocean heat transport divergence relative to that of 2CO2 to keep the sea surface temperatures cooler than in 2CO2. Neither the GISS nor the GFDL doubled CO_2 equilibrium experiments allow ocean heat transport divergence relative to their control run. For the GFDL experiment to produce a small low latitude ocean temperature response indicates that either the altered surface energy flux, especially the evaporative loss, for a given change in ocean temperature is greater than in the GISS model (and, as noted earlier, the fine grid GISS runs have greater

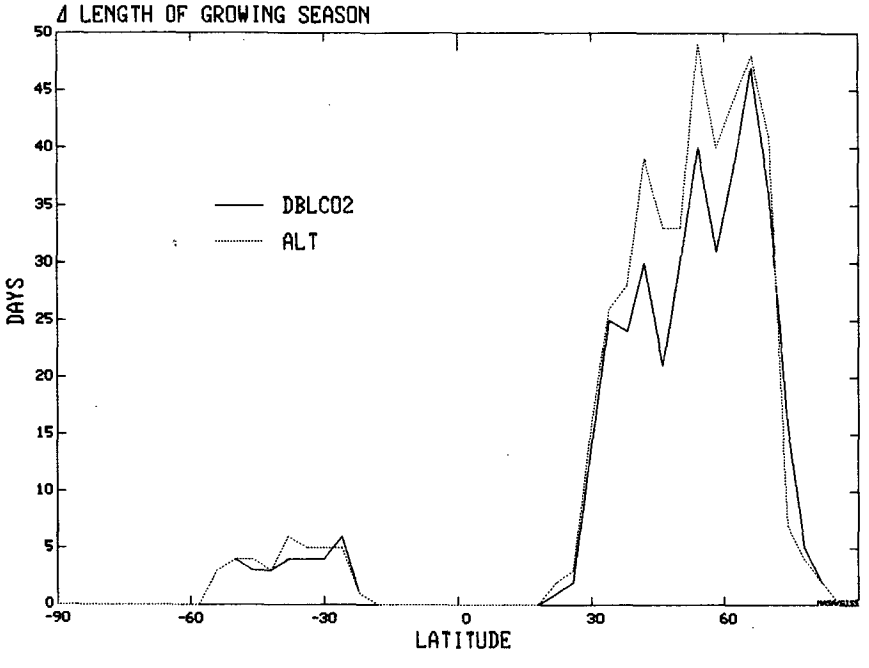

FIG. 23. Change in the length of the growing season (successive days between frosts) for 2CO2 minus control (solid line) and ALT minus control (dotted line).

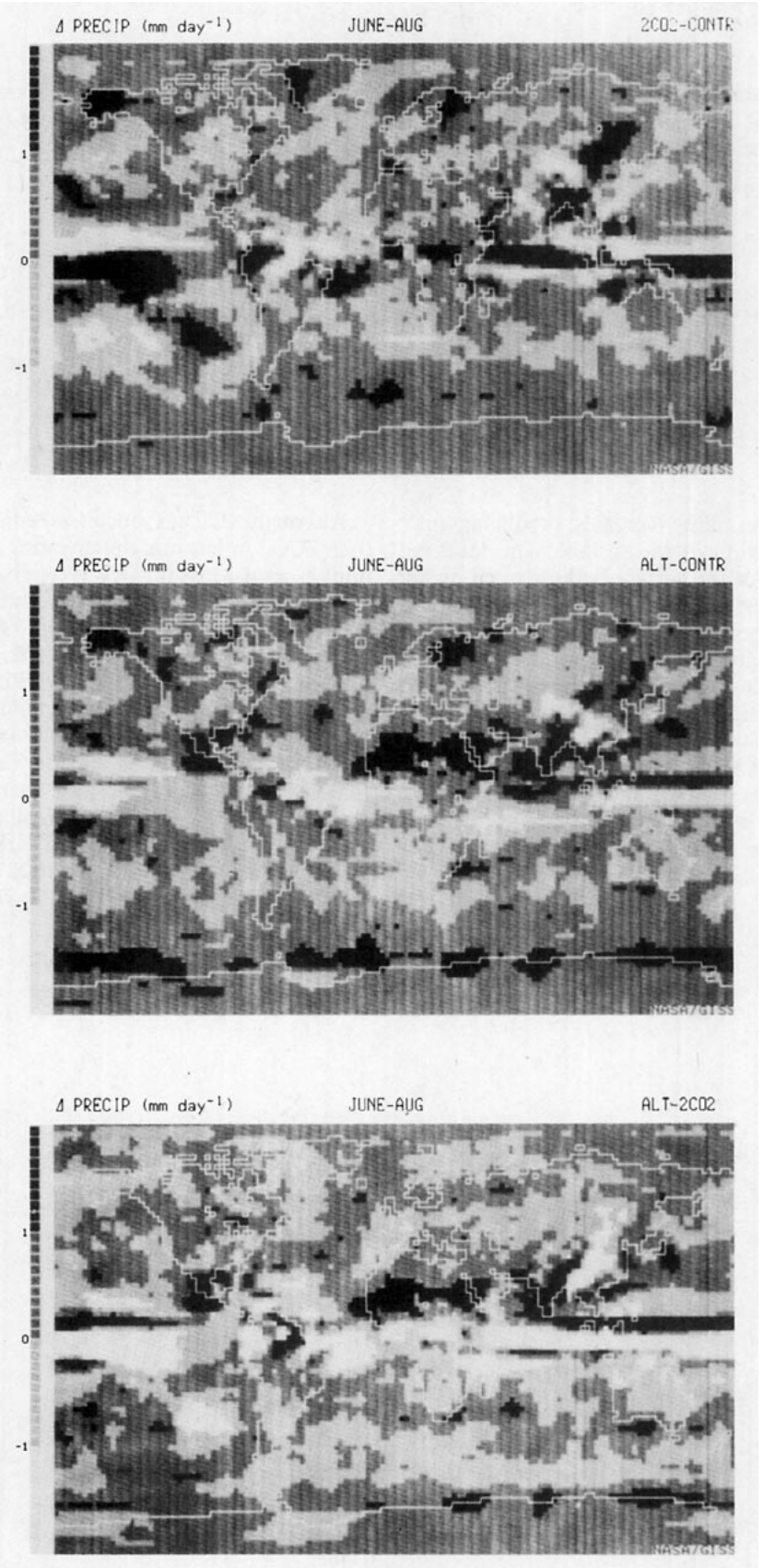

FIG. 24. Change in precipitation for the three years, June–August, for 2CO2 minus control, ALT minus control, and ALT minus 2CO2.

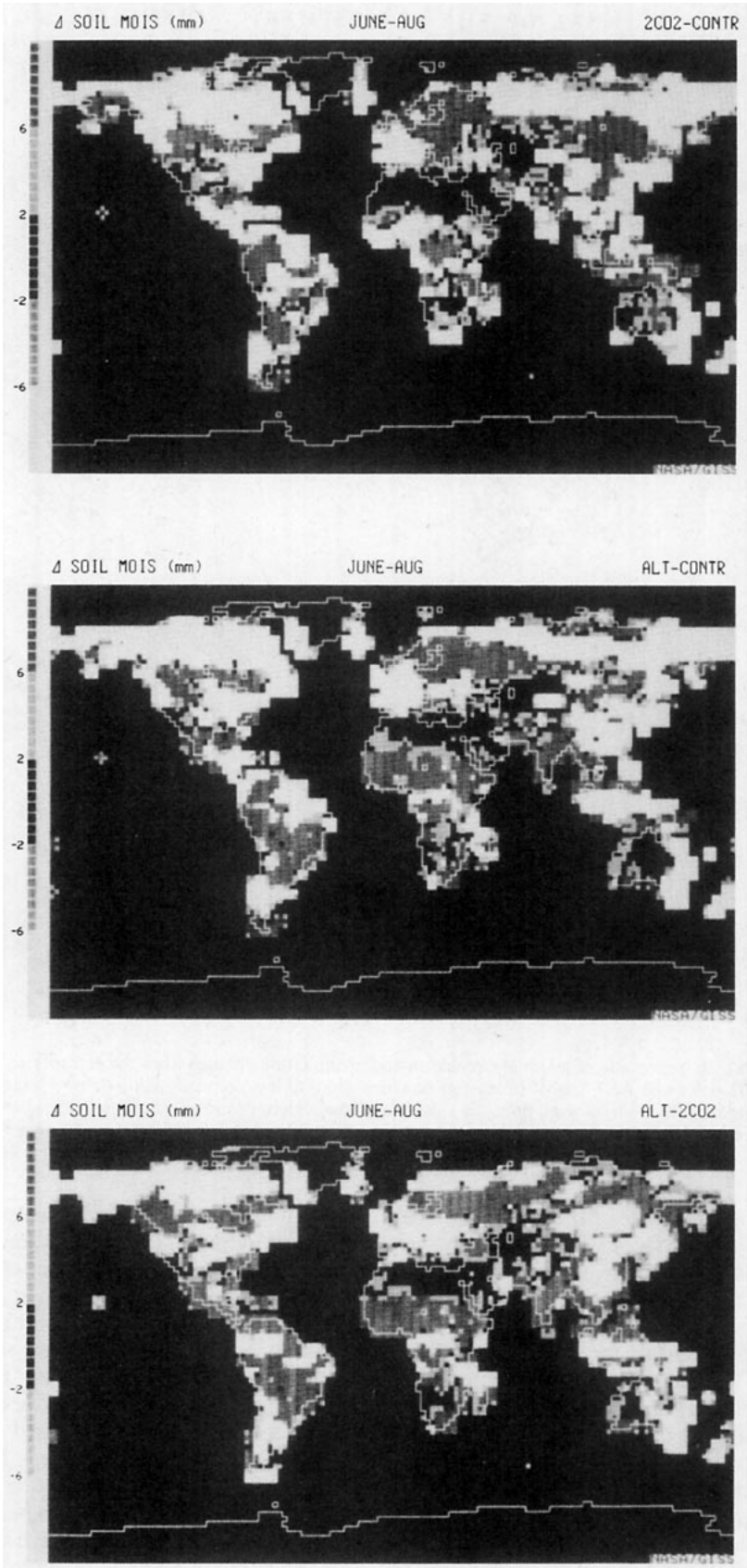

FIG. 25. Change in soil moisture from the third year, June–August, for 2CO2 minus control, ALT minus control, and ALT minus 2CO2.

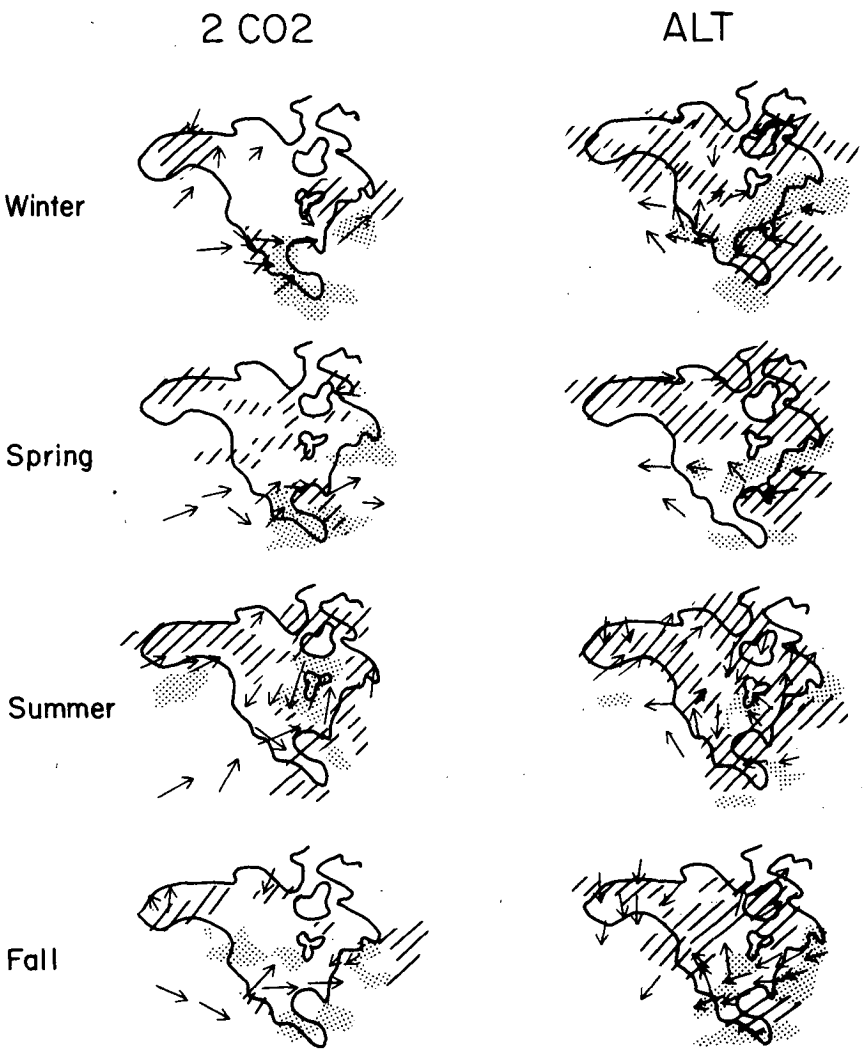

FIG. 26. Schematic of seasonal circulation and precipitation changes from the control run for 2CO2 (left) and ALT (right) (from top down: winter, spring, summer, fall). Arrows indicate change in 200 mb level wind flow, diagonal lines show regions of increased rainfall, dotted areas decreased rainfall. Only regions with precipitation change greater than 0.5 mm d^{-1} are shown.

evaporative loss than the coarse grid runs), or the net radiative heating of the surface is smaller (both processes would eliminate the net heating and the need for the ocean heat transport divergence required in ALT). The surface evaporative response depends upon the magnitude of the sea surface temperatures (and the GFDL control run for the doubled CO_2 experiment referred to above does not have any ocean heat transport) as well as the surface layer parameterization and atmospheric transport of moisture away from the low latitude surface, while the radiative response is a function of the hydrologic cycle (evaporation, convection, cloud cover, dynamical moisture transport) and radiation scheme. Systematic studies would be required to isolate which if any of these processes are responsible for the models' different low latitude warming.

What about the high latitude response? The surface temperature in ALT would, in general, cool if allowed to adjust, due to the large surface energy loss associated with decreased sea ice. Hansen et al. (1984) described an alternate doubled CO_2 experiment run with a different formulation for sea ice, one which produced more sea ice in the control run. This change then allowed for a greater sea ice reduction in the doubled CO_2 experiment, and it increased the high latitude response by about 0.5°C. The sea ice change is thus a factor in the degree of high latitude warming. However, while the difference in these experiments at high latitudes was initiated by the change in sea ice, additional warming (relative to the standard doubled CO_2 run) occurred at all latitudes. The increase in high latitude warming at equilibrium was similar to the global av-

TABLE 4. Change in annual hydrologic balance over ice sheets (mm d^{-1}).

Area		Change in ΔPrecipitation	ΔEvaporation	ΔRunoff	ΔIce
Greenland	2CO2-Control	0.4	0	1.8	−1.4
	ALT-Control	0.5	0.2	2.8	−2.5
Antarctica					
70°S	2CO2-Control	0.4	0	1.0	−0.6
	ALT-Control	0.9	0	2.4	−1.5
74°S	2CO2-Control	0.4	0	0.5	−0.1
	ALT-Control	0.6	0	0.9	−0.3
78°S	2CO2-Control	0.3	0	0.4	−0.1
	ALT-Control	0.4	0	0.6	−0.2
82°S	2CO2-Control	0.2	0	0.7	−0.5
	ALT-Control	0.3	0	0.8	−0.5
86°S	2CO2-Control	0.2	0	0	0.2
	ALT-Control	0.3	0	0	0.3

erage change, and so the high latitude amplification did not increase. Note that the high latitude response is apparently not limited by the atmospheric latitudinal energy transports: as shown above, the GISS model response to increased CO_2 is to increase atmospheric energy transport to high latitudes, while the GFDL model has less poleward energy transport with increased CO_2 (Manabe and Wetherald, 1980). If the results from 2CO2 and ALT are relevant, the model transport differences are due to the difference in high latitude amplification and are working to reduce them. Differences between the GISS model and the GFDL model sea ice formation, ocean transports, cloud generation, and convection (which removes heat from the surface) are the most likely reasons for the different high latitude responses.

b. Atmospheric dynamics

A previous paper (Rind, 1986) compared the changes in atmospheric dynamics that occurred in different climate simulations. The climates involved were characterized by differences in sea surface temperature, sea surface temperature gradients, and topography. It was thus difficult to determine which aspect was responsible for the changes that did occur. The results presented here, in combination with those given in Rind (1986, 1987), allow for a separation of the various influences. The following are the major conclusions that can be drawn from the different studies.

1) *The Hadley Cell intensity varies with the low latitude sea surface temperature gradient, not the absolute value of the sea surface temperature.*

ALT has warmer sea surface temperatures than the control run, yet a weaker Hadley Cell. This occurred because the region of highest equatorial sea surface temperatures received less of an increase than did other areas; for example, the December–February sea surface temperature change with latitude from 2°S to 14°N in the control run was 1.5°C (28.5° to 27°C), while in ALT it was only 0.6°C (30.0° to 29.4°). A similar decrease in equatorial temperature gradient and Hadley Cell intensity occurred in the Mesozoic climate experiment (Rind, 1986). The ice age experiments had low latitude sea surface temperature gradients similar to those of the present climate, and similar Hadley Cell intensities (Rind, 1986, 1987), even though the tropical ocean temperatures were cooler. The 2CO2 had slightly greater warming at the equator than at neighboring latitudes and a slightly stronger Hadley Cell. This result is due to the influence of the sea surface temperature pattern on the rainfall distribution. An equatorial rainfall peak drives a stronger Hadley circulation through its influence on the thermally forced portion of the Hadley Cell (i.e., transformed streamfunction); similarly, an equatorial sea surface temperature minimum reduces equatorial rainfall and diminishes the Hadley Cell. CISK feedbacks are likely important here, and the circulation cells developed appear to have a width of about 10°–20° latitude.

2) *The changes in Hadley Cell intensity between the different climates are relatively small, despite the relatively large changes in equatorial precipitation.*

This is likely the result of the influence of the other major thermal forcing of the Hadley circulation, solar absorption peaking during the solstices at 23° latitude. The equatorial and subtropical heat sources are out of phase, and the combination acts to limit the Hadley Cell intensity compared to what occurs (in the model) when solar radiation absorption is absent (Rind and Rossow, 1984). As the solar influence is similar in all the climate simulations, it limits the change in Hadley Cell intensity and its sensitivity to low latitude sea surface temperature gradient changes.

3) *The Hadley Cell northward extent varies little in the climate change experiments, due to compensating*

effects between eddy heat transports and the hydrologic cycle.

Both ALT and 2CO2 have reduced eddy energy and reductions in the eddy-induced indirect midlatitude streamfunction. Yet this does not result in much extension of the Hadley Cell to higher latitudes, in contrast to the results of Rind and Rossow (1984), who found the Hadley Cell extent did depend on the (more extreme) variations in eddy energy. Associated with the decreased latitudinal temperature gradient, responsible for the weaker eddies, are warmer temperatures, greater moisture availability, increased eddy latent heat transport to higher latitudes, and greater high latitude rainfall. The increased high latitude latent heat release results in an indirect, thermally induced streamfunction that effectively compensates for the change due to the weaker eddies. The reverse situation, stronger eddies but less high latitude rainfall, occurs in the ice age experiments (Rind, 1986, 1987) with, again, little change in Hadley Cell northward extent. It is not obvious that the compensation need be perfect, and it may allow for small shifts in the location of Hadley Cell descent that would have important climatological consequences. Model simulations would need to be run with very fine horizontal resolution to produce such an effect, and limitations on the realism of different parameterizations would induce uncertainty into the balances obtained (Rind and Rossow, 1984).

4) *The subtropical jet stream maintains consistency with the thermal wind relationship, but the nature of the balance that produces this consistency changes with different climate simulations.*

ALT experienced a decrease in the latitudinal temperature gradient, which, as implied by the thermal wind relationship, resulted in a decrease in jet stream intensity. The change was primarily the result of reduced momentum convergence by the mean circulation. The 2CO2 experienced an increase in jet stream intensity, influenced by a reduction in stationary eddy deceleration of the jet. In the ice age experiments, stationary eddies were actually accelerating the jet (Rind, 1987). The mean circulation, eddies, and friction play almost equal roles in the model's momentum balance at the jet stream level, and the importance of each component varies with the climate (Rind, 1986). In other words, the maintenance of geostrophic and hydrostatic equilibrium is provided by different processes in different climate regimes; there can be increases in eddy energy with no jet stream change (as in the ice age experiments) and decreases in eddy energy with either jet stream decrease or increase (ALT versus 2CO2).

5) *The ratio of stationary to transient eddy energy depends on the land–ocean temperature contrast and the latitudinal temperature gradient.*

Processes that cool the continents in winter (such as increased topography in the ice age experiments) or warm the ocean in winter (such as specified warmer sea surface temperatures) will *tend* to increase the stationary wave energy by deepening the climatological winter ocean low-pressure systems. Whether the stationary eddy energy actually does increase depends also on the latitudinal temperature gradient. In the full ice age experiment, both the land–ocean contrast and the latitudinal temperature gradient increase, and so does the stationary eddy energy. [The ice age topographic forcing of stationary waves also increased in this experiment, but as discussed (Rind, 1987), with broad ice sheets it is difficult to separate the ice sheet thermal effect—due to the reduced atmospheric greenhouse capacity above—from the pure topographic influence investigated by Manabe and Terpstra (1974).] In ALT the land–ocean contrast increased due to the warmer ocean waters, but the latitudinal temperature gradient decreased, so the stationary eddy energy remained nearly constant. In 2CO2 the land–ocean contrast showed little change, but the latitudinal temperature gradient decreased, as did the stationary eddy energy. In an ice age experiment with the ice age sea surface temperature distribution but no additional land ice topography, the latitudinal temperature gradient increased but the stationary wave energy decreased, as the colder mid- and high latitude ocean waters stabilized the regions of climatological low pressure (Rind, 1987).

The transient eddy energy responds directly to the latitudinal temperature gradient, increasing when this gradient increases, but the magnitude of the change depends on what happens to the stationary eddies. With decreased land–ocean contrast, eddies move in different storm tracks, producing more transient and less stationary eddy energy. Thus, when the latitudinal temperature gradient increases and the land–ocean contrast decreases, as in the ice age experiment with just the altered sea surface temperatures, very large increases in transient eddy energy occur (Rind, 1987). When the latitudinal temperature gradient decreases but the land–ocean contrast remains high, transient eddy energy decreases strongly, as in ALT. In the climate simulations discussed by Rind (1986) the ratio of transient to stationary eddy energy was surprisingly constant; in those cases, both the land–ocean contrast (of both temperature and topography) and the latitudinal temperature gradient tended to change in the same sense (increases in both during the ice age, decreases in both during the Mesozoic, smaller decreases in both for doubled CO_2).

6) *Changes in the available potential energy do not necessarily lead to the expected changes in baroclinic instability.*

It is normally assumed that changes in the zonal available potential energy (A_z), representative of the latitudinal temperature gradient, will be followed by similar changes in the eddy available potential energy (A_e) and baroclinic energy conversion to eddy kinetic energy (K_e), but such is not the case in the model runs with specified sea surface temperature changes. When

the ice age sea surface temperatures were input into the GISS model, increases of A_z of 10% occurred, while A_e decreased by a similar amount, and baroclinic energy conversion from A_e to eddy kinetic energy showed little change. The cold ocean waters enforced the A_e decrease and overcame the effects of the increased latitudinal temperature gradient. However, the colder ocean waters were apparently associated with greater barotropic energy transfer, so K_e increased along with A_z, without changes in A_e or $A_e \rightarrow K_e$.

The value A_z was substantially less in ALT than in 2CO2, but A_e was larger; here the warm ocean waters in ALT helped maintain A_e, although there was a large decrease in the latitudinal temperature gradient. Despite the large A_e, ALT showed a large decrease in baroclinic instability. Changes in the different components of the energy cycle cannot foretell with certainty how energy transfers or other components will change, as the (model) atmosphere alters the nature of energy conversion and the eddy characteristics in response to the given latitudinal and longitudinal makeup of the particular climate regime.

7) *The total energy transports do not provide a consistent feedback to the climate change.*

Energy balance models (e.g., Saltzman, 1978) assume that as the latitudinal temperature gradient changes, energy transports will change in the same sense, for example, decreasing in warm climates with high latitude temperature amplification. The transports are thus expected to provide a negative feedback to the climate change tendency. The model results do not indicate a consistent sign to this feedback, especially when the implicit ocean transports are included. Ice age experiments in general showed increasing transports in the colder climate, although the climate with the greatest latitudinal temperature gradient did not have the largest transport (Rind, 1987). The 2CO2 had greater atmospheric transports than did the control, even though it was a warmer climate with some high latitude temperature amplification. ALT had smaller atmospheric transports, but greater total transports when the implied ocean effects were included. One reason for the difference in the model results from expectations is that the transport of water vapor is often neglected in estimates of how energy transports will change with climate; with warm equatorial waters and greater moisture availability, positive dynamical feedbacks are possible. In addition, the influence of longitudinal variations on atmospheric dynamics affects energy transports, as indicated by the variety of responses in the energy cycle shown by the different climates to A_z changes.

c. *Regional changes*

The consistent results obtained in doubled CO_2 experiments with different versions of the GFDL model, as well as the "dust bowl" droughts of the relatively warm 1930s, have led to expectations of reductions in soil moisture over the United States as climate warms. The results presented here indicate that the magnitude of the change may well depend upon the degree of high latitude amplification that actually occurs, particularly the degree of warming in the midlatitudes. It is interesting that both the GISS and NCAR models produce the same magnitude of high latitude amplification, less than one-half that of the GFDL model, and neither develops the ubiquitous Northern Hemisphere drying seen in the GFDL results. The UKMO model produced general midlatitude drying with both a uniform sea surface temperature change and a temperature change increasing with latitude (Mitchell and Lupton, 1984), although it is difficult to compare the relative magnitudes of the drying in the runs since the temperature changes were a factor of two different. Additional doubled CO_2 experiments have been run recently with the UKMO model (Wilson et al., 1987) and the OSU model (Schlesinger and Zhao, 1987). Both produce midlatitude drying without the magnitude of high latitude amplification in summer that occurred in ALT. Both also have greater high latitude amplification than the GISS model in general, and this will influence the timing and magnitude of snow melt and runoff. Early spring melt and runoff, aided by high latitude warming, is a factor in producing midlatitude summer soil moisture decreases in the different models. This result emphasizes that the seasonal variation of high latitude amplification is also important to regional hydrologic results. Additional differences among models probably arise due to their use of different ground hydrology parameterizations and to differences in convection schemes.

Other regional results are also sensitive to the sea surface temperature gradient. At lower latitudes, rainfall changes dominate the resulting changes in water availability and are particularly sensitive to the degree of low latitude warming. At high latitudes, potential ice sheet melting increases with high latitude warming, as increased runoff exceeds increased precipitation. We do not yet understand the reasons behind the different degrees of high latitude amplification or low latitude warming produced in the different models; with uncertainties still existing as to what the paleoclimate record indicates about low latitude changes, it is not possible to decide which model is more accurate. It is also very likely that the soil moisture change results will depend strongly on the ground hydrology model used in the GCMs; current models are very simplistic. The opinion here is that a substantial decrease in midlatitude soil moisture due to doubled CO_2 warming cannot be said to be a foregone conclusion. However, over the United States, similarities do exist in the height field changes in 2CO2 and ALT. This implies that certain regional climate change assessments may be possible, even with the existing uncertainties in the change in latitudinal temperature gradient.

Acknowledgments. Reto Reudy graciously provided assistance in obtaining the necessary diagnostic output and overseeing the running of these experiments. Climate modeling at GISS is supported by the NASA Climate Program Office.

REFERENCES

Andrews, D. G., and M. E. McIntyre, 1976: Planetary waves in horizontal and vertical shear. The generalized Eliassen–Palm relation and the mean zonal acceleration. *J. Atmos. Sci.*, **33,** 2031–2048.

Barth, C. M., and J. G. Titus, Eds., 1984: *Greenhouse Effect and Sea Level Rise.* Van Nostrand Reinhold, 325 pp.

CLIMAP Project Members (A. McIntyre, project leader), 1981: Seasonal reconstruction of the earth's surface at the last glacial maximum. *Geol. Soc. Amer.,* Map and Chart Ser., No. 36.

Dunkerton, T., 1978: On the mean meridional mass motions of the stratosphere and mesosphere. *J. Atmos. Sci.*, **35,** 2325–2333.

Edmon, H. J., Jr., B. J. Hoskins and M. E. McIntyre, 1980: Eliassen–Palm cross sections in the troposphere. *J. Atmos. Sci.*, **37,** 2600–2616.

Eliassen, A., and E. Palm, 1961: On the transfer of energy in stationary mountain waves. *Geophys. Publ.*, **22,** 1–23.

Frakes, L. A., 1979: *Climates throughout Geologic Time.* Elsevier, 310 pp.

Gray, W. M., 1984: Atlantic seasonal hurricane frequency. Part I: El Niño and 30 mb quasi-biennial oscillation influences. *Mon. Wea. Rev.*, **112,** 1649–1668.

Green, J. S. A., 1960: A problem in baroclinic instability. *Quart. J. Roy. Meteor. Soc.*, **86,** 237–251.

Hansen, J., G. Russell, D. Rind, P. Stone, A. Lacis, S. Lebedeff, R. Reudy and L. Travis, 1983: Efficient three-dimensional global models for climate studies: Models I and II. *Mon. Wea. Rev.*, **111,** 609–662.

——, A. Lacis, D. Rind, G. Russell, P. Stone, I. Fung, R. Ruedy and J. Lerner, 1984: Climate sensitivity: Analysis of feedback mechanisms. *Climate Processes and Climate Sensitivity,* J. Hansen and T. Takahashi, Eds., Amer. Geophys. Union, 130–163.

Lau, N.-C., 1985: Modeling the seasonal dependence of the atmospheric response to observed El Niños in 1962–1976. *Mon. Wea. Rev.*, **113,** 1970–1996.

Manabe, S., and T. B. Terpstra, 1974: The effects of mountains on the general circulation of the atmosphere as identified by numerical experiments. *J. Atmos. Sci.*, **31,** 3–42.

——, and R. T. Wetherald, 1980: On the distribution of climate change resulting from an increase of CO_2 content of the atmosphere. *J. Atmos. Sci.*, **37,** 99–118.

——, —— and Stouffer, R. J., 1981: Summer dryness due to an increase of atmospheric CO_2 concentration. *Climate Change,* **3,** 347–386.

——, and K. Bryan, Jr., 1985: CO_2-induced change in a coupled ocean atmosphere model and its paleoclimatic implications. *J. Geophys. Res.*, **90,** 11 689–11 707.

——, and R. T. Wetherald, 1986: Reduction in summer soil wetness induced by an increase in atmospheric carbon dioxide. *Science,* **232,** 626–628.

Manabe et al., 1981:

Meier, M. F., Ed., 1985: *Glaciers, Ice Sheets, and Sea Level: Effect of a CO_2-Induced Climatic Change.* U.S. Dept. of Energy, DOE/ER/60235-1, Washington, DC, 348 pp.

Mitchell, J. F. B., 1983: The seasonal response of a general circulation model to changes in CO_2 and sea temperature. *Quart. J. Roy. Meteor. Soc.*, **109,** 113–152.

——, and G. Lupton, 1984: A 4 × CO_2 integration with prescribed changes in sea surface temperatures. *Prog. Biometeor.*, **3,** 353–374.

——, C. A. Wilson and W. M. Cunnington, 1987: On CO_2 and clouds: Mechanisms of cloud changes due to tropospheric warming. Chapter 2, Final Rep. CEC Contract CL-114-UK (H), British Meteorological Office, Bracknell, U.K.

Rind, D., 1986: The dynamics of warm and cold climates. *J. Atmos. Sci.*, **43,** 3–24.

——, 1987: Components of the ice age circulation. *J. Geophys. Res.*, **92,** 4241–4281.

——, and W. Rossow, 1984: The effects of physical processes on the Hadley circulation. *J. Atmos. Sci.*, **41,** 479–507.

——, and D. Peteet, 1985: Terrestrial conditions at the last glacial maximum and CLIMAP sea-surface temperature estimates: Are they consistent? *Quat. Res.*, **24,** 1–22.

Saltzman, B., 1970: Large-scale atmospheric energetics in the wavenumber domain. *Rev. Geophys. Space. Physics,* **8,** 289–302.

——, 1978: A survey of statistical–dynamical models of the terrestrial climate. *Advances in Geophysics,* Vol. 20, Academic Press, 183–295.

Schlesinger, M. E., and J. F. B. Mitchell, 1985: Model projections of the equilibrium climatic response to increased carbon dioxide. *The Potential Climatic Effects of Increasing Carbon Dioxide,* M. C. MacCracken and F. M. Luther, Eds., DOE/ER-0237, U.S. Dept. of Energy, Washington, DC, 81–148.

——, and ——, 1987: Model projections of the equilibrium climatic response to increased CO_2. *Rev. Geophys.* (in press).

——, and Z. Zhao, 1987: Seasonal climate changes induced by doubled CO_2 as simulated by the OSU atmospheric GCM/mixed layer ocean model. Oregon State University Climatic Institute Rep. 70, 73 pp.

——, W. L. Gates and Y.-J. Han, 1985: The role of the ocean in the CO_2-induced climate warming: Preliminary results from the OSU coupled atmosphere–ocean GCM. *Coupled Ocean–Atmosphere Models,* J. C. J. Nihoul, Ed., Elsevier, 447–478.

Washington, W. M., and G. A. Meehl, 1984: Seasonal cycle experiment on the climate sensitivity due to a doubling of CO_2 with an atmospheric general circulation model coupled to a simple mixed-layer ocean model. *J. Geophys. Res.*, **89,** 9475–9503.

Wetherald, R. T., and S. Manabe, 1980: Cloud cover and climate sensitivity. *J. Atmos. Sci.*, **37,** 1485–1510.

Wilson, C. A., J. F. B. Mitchell and W. M. Cunnington, 1987: A 2 × CO_2 climate sensitivity experiment with a global climate model including a simple ocean. Chapter 3, Final Rep. CEC Contract CL-114-UK (H), British Meteorological Office, Bracknell, U.K.